

Spring 1-1-2014

Calibration of Capacitance Sensors for Use in Nonisothermal Applications

Hannah Maria Iezzoni

University of Colorado at Boulder, hannah.iezzoni@colorado.edu

Follow this and additional works at: https://scholar.colorado.edu/cven_gradetds



Part of the [Geotechnical Engineering Commons](#)

Recommended Citation

Iezzoni, Hannah Maria, "Calibration of Capacitance Sensors for Use in Nonisothermal Applications" (2014). *Civil Engineering Graduate Theses & Dissertations*. 148.

https://scholar.colorado.edu/cven_gradetds/148

This Thesis is brought to you for free and open access by Civil, Environmental, and Architectural Engineering at CU Scholar. It has been accepted for inclusion in Civil Engineering Graduate Theses & Dissertations by an authorized administrator of CU Scholar. For more information, please contact cuscholaradmin@colorado.edu.

CALIBRATION OF CAPACITANCE SENSORS
FOR USE IN NONISOTHERMAL APPLICATIONS

by

HANNAH MARIA IEZZONI

B.S. Northwestern University, 2012

A thesis submitted to the
Faculty of the Graduate School of the
University of Colorado in partial fulfillment
of the requirement for the degree of
Master of Science
Department of Civil, Environmental and Architectural Engineering

2014

This thesis entitled:

Calibration of Capacitance Sensors for Use in Nonisothermal Applications

written by Hannah Maria Iezzoni

has been approved for the Department of Civil, Environmental and Architectural Engineering

Professor John S. McCartney (committee chair)

Professor Dobroslav Znidarčič

Professor Shideh Dashti

Date_____

The final copy of this thesis has been examined by the signatories, and we
Find that both the content and the form meet acceptable presentation standards
Of scholarly work in the above mentioned discipline

Iezzoni, Hannah Maria (M.S. Civil Engineering, Department of Civil, Environmental and Architectural Engineering)

Calibration of Capacitance Sensors for Use in Nonisothermal Applications

Thesis directed by Professor John S. McCartney

ABSTRACT

This study investigates how temperature affects the response of capacitance sensors. These sensors are used to measure the dielectric permittivity of unsaturated soils, which is a useful variable to characterize, as it is strongly related to the volumetric water content. The volumetric water content is frequently used in the analyses of water flow through soils. Capacitance sensors have been used in experiments intended to characterize thermally-induced flow of water in unsaturated soils during geothermal heat exchange processes. Water flow is an important process in the design of thermally-active geotechnical systems such as energy piles and thermally-active retaining walls. To date, no studies have characterized the effect of temperature on capacitance sensor output from a geotechnical perspective (where soils are typically dense). An understanding of this topic is necessary to obtain an accurate estimate of thermally-induced changes in volumetric water content in thermally active geotechnical systems.

This paper describes the heating experiments performed on compacted soil layers with constant water content that indicated changes in temperature can lead to changes in the measured dielectric permittivity of up to 40%. The capacitance sensor's response to changing temperatures was observed to be sensitive to the initial density of the soil, but not to the initial volumetric water content for soils compacted at a constant density. A calibration equation to consider the soil-specific relationship between volumetric water content and dielectric permittivity was defined, along with a correction equation to account for temperature effects in unsaturated soils having different dry density values.

ACKNOWLEDGEMENT

The author wishes to thank her advisor, Professor John Scott McCartney, for facilitating this research opportunity. Special recognition is given to the members of the thesis committee, Professors Dobroslav Znidarčić and Shideh Dashti, who have provided valuable feedback on this work. In addition, a special thank you is offered to the many geotechnical graduate students who helped keep this project moving forward with their enthusiasm and positivity, especially Melissa Stewart, Lauren Reising, CJ Coccia, David Provost and Kenneth Gillis. Most importantly the author extends her appreciation, gratitude and love to her incredibly supportive family and the wonderful Erik Hamilton. Funding from NSF grant CMMI 1230237 is greatly appreciated.

TABLE OF CONTENTS

| | |
|---|----|
| 1. Introduction | 1 |
| 1.1. Motivation | 1 |
| 1.2. Problem Statement | 2 |
| 1.3. Objective | 3 |
| 1.4. Approach | 3 |
| 1.5. Scope | 4 |
| 2. Background and Literature Review | 5 |
| 2.1. Water Retention in Unsaturated Soils | 5 |
| 2.1.1. Expressions for Water Content | 5 |
| 2.1.2 Matric Suction and the Soil Water Retention Curve | 6 |
| 2.2 Electromagnetic Properties | 7 |
| 2.2.1 Overview | 7 |
| 2.2.2 Electrical Conductivity | 8 |
| 2.2.3 Magnetic Permeability | 8 |
| 2.2.4 Dielectric Permittivity | 8 |
| 2.3 Water Content Sensors | 9 |
| 2.3.1 Overview | 9 |
| 2.3.2 Soil Moisture Neutron Probe | 9 |
| 2.3.3 Electrical Resistivity Probes | 9 |
| 2.3.3 Dielectric Sensors | 10 |
| 2.3.3.1 Time Domain Reflectometry (TDR) | 10 |
| 2.3.3.2 Frequency Domain Reflectometry (FDR) | 10 |
| 2.4 Variables that Affect Electromagnetic Measurements | 11 |

| | |
|---|----|
| 2.4.1 Texture and Soil Fabric | 11 |
| 2.4.2 Operation Frequency | 12 |
| 2.4.3 Temperature | 13 |
| 2.5 Previous Calibration Tests | 14 |
| 3. Materials | 16 |
| 3.1. Overview | 16 |
| 3.2. Geotechnical Characterization | 16 |
| 3.2.1.Overview | 16 |
| 3.2.2. Hydraulic Properties | 18 |
| 3.2.3. Thermal Properties | 20 |
| 4. Experimental Approach and Methodology | 21 |
| 4.1. Overview | 21 |
| 4.2. Compaction Mold | 21 |
| 4.3. Instrumentation | 22 |
| 4.4. Soil Layer Preparation | 23 |
| 5. Experimental Results | 25 |
| 5.1. Overview | 25 |
| 5.2. Baseline Test Results | 25 |
| 5.3. Evaluation of the Impact of Heat Duration Test Results | 27 |
| 5.3.1. Overview | 27 |
| 5.3.2. Time Series Data | 28 |
| 5.3.3. Water Content Profiles Before and After Heating | 29 |
| 5.4. Evaluation of the Impact of Initial Water Content | 31 |
| 5.4.1. Overview | 31 |

| | |
|--|----|
| 5.4.2. Time Series Data | 32 |
| 5.5. Evaluation of the Impact of Initial Dry Density | 33 |
| 5.5.1. Overview | 33 |
| 5.5.2. Time Series | 34 |
| 6. Analysis | 35 |
| 6.1. Overview | 35 |
| 6.2. Ambient Temperature Calibration Curve | 35 |
| 6.3. Impact of the Initial Water Content on the Temperature Effect | 35 |
| 6.4. Impact of Initial Dry Density on the Temperature Effect | 39 |
| 6.5. Correction Equation for Temperature Effects | 40 |
| 7. Conclusion | 42 |
| References | 43 |

LIST OF TABLES

| | |
|---|----|
| Table 3.1: Grain size distribution data for Bonny silt | 17 |
| Table 3.2: Atterberg limits for Bonny silt | 17 |
| Table 4.1: Sample compaction condition details for the 3-hour test #1 | 24 |
| Table 5.1: Compaction details for tests with varying duration of heating | 28 |
| Table 5.2: Compaction details for tests with varying initial water contents | 32 |
| Table 5.3: Compaction details for tests with varying initial water contents | 33 |

LIST OF FIGURES

| | |
|---|----|
| Figure 2.1: Drying-paths SWRCs for different geotechnical materials (McCartney 2007) | 7 |
| Figure 2.2: The dielectric permittivity of water as a function of temperature (Malmberg and Maryott 196) | 13 |
| Figure 3.1: Grain size distribution curve for Bonny silt | 17 |
| Figure 3.2: Compaction curves for Bonny silt obtained using both standard and modified Proctor compaction efforts, plotted with the zero air void (ZAV) line | 18 |
| Figure 3.3: Hydraulic conductivity as a function of void ratio for Bonny silt | 19 |
| Figure 3.4: SWRCs for Bonny silt specimens having an initial void ratio of 0.69 under a range of net stresses (Khosravi 2012) | 19 |
| Figure 3.5: Relationship between thermal conductivity and void ratio for Bonny silt | 20 |
| Figure 4.1: Schematic of the compaction mold used for all experiments. Shows rubber stopper plug used to seal sensor wire exiting mold and the location of the sensor (and its zone of influence) after compaction. | 22 |
| Figure 4.2: The initial conditions of all tests plotted over the Proctor curves for Bonny silt | 24 |
| Figure 5.1: Results from the baseline test on a sensor in air plotted as the measured temperature versus the apparent dielectric permittivity | 26 |
| Figure 5.2: The time series data from the baseline tests showing the sensor response in a fully dry and fully saturated sample to a) temperature and b) dielectric permittivity | 27 |
| Figure 5.3: The baseline tests results showing the changes in temperature as a function of dielectric permittivity | 27 |
| Figure 5.4: The time series data from the tests evaluating heating duration showing the sensor response to a) temperature and b) dielectric permittivity | 29 |
| Figure 5.5: Location of gravimetric water content samples taken to check water migration | 30 |
| Figure 5.6: Profiles of gravimetric water content samples taken from each lift during compaction and after heating for different durations | 31 |
| Figure 5.7: A plot the calculated volumetric water content values versus the | 31 |

corresponding volumetric water content values measured by the sensor (calibrated from the dielectric permittivity measurements using Topp's equation).

- Figure 5.9: The effect of initial dry density on the time series data for: (a) Temperature; (b) Apparent dielectric permittivity. 3
- Figure 5.10: The effect of initial dry density on the time series data for: a) temperature and b) apparent dielectric permittivity 33
- Figure 6.1: Soil specific calibration curves developed for measuring dielectric permittivity of Bonny silt at different initial dry densities using a capacitance sensor. 36
- Figure 6.2: The "A" factor (the slope of the linear relationship between dielectric permittivity and volumetric water content) as a function of the initial dry density. 37
- Figure 6.3: Impact of initial water content on the capacitance sensor temperature effects: (a) Temperature versus apparent dielectric permittivity; (b) Change in temperature versus change in apparent dielectric permittivity. 38
- Figure 6.4: Slope of the temperature effect curves for the capacitance sensor for each test plotted against the initial volumetric water content. 38
- Figure 6.5: Impact of initial dry density on the capacitance sensor temperature effects: (a) Temperature versus apparent dielectric permittivity; (b) Change in temperature versus change in apparent dielectric permittivity. 39
- Figure 6.6: The rate of change in dielectric permittivity with change in temperature for each test plotted against the initial dry density. 40
- Figure 6.7: The rate of change in dielectric permittivity with change in temperature for each test plotted against the (a) initial volumetric water content and (b) initial dry density. 41
- Figure 6.8: Example of the application of the temperature correction equation. 41

CHAPTER 1

INTRODUCTION

1.1 Motivation

Thermally-active geotechnical systems are created by incorporating geothermal heat exchangers into civil engineering infrastructure such as building foundations, embankments, or retaining walls (Coccia and McCartney 2013; Stewart et al. 2014; Murphy and McCartney 2014). If the compacted soil backfill used in these systems is unsaturated, heating and cooling of the soil may lead to thermally-driven water flow (Philip and DeVries 1957). This thermally-driven water flow process may have significant effects on both the thermal properties (Smits et al. 2013) and the mechanical response of unsaturated soils (Coccia and McCartney 2013; Coccia et al. 2013; Stewart et al. 2014). Accordingly, it is important to have a technique to infer transient changes in volumetric water content around geothermal heat exchangers in unsaturated soil. If it is possible to accurately infer thermally-induced changes in volumetric water content of unsaturated soils using such a technique, then this information can be used to calibrate or validate numerical simulations of heat and water flow processes. Calibration of these numerical simulations is particularly necessary due to coupling between changes in temperature and changes in volumetric water content. Validated numerical simulations are needed to accurately design thermally active geotechnical systems.

Dielectric sensors have been used for many years to infer the volumetric water content of unsaturated soils at a point by inferring the bulk dielectric permittivity of the soil, which is closely related with the amount of water in the soil. Although dielectric sensors come in many forms (time domain reflectometry, frequency domain reflectometry, water content reflectometers, capacitance sensors, etc.), capacitance sensors are the most cost-effective dielectric sensor with the simplest data acquisition system. Despite these advantages, the effects

of temperature on the response of capacitance sensors has not been well characterized for compacted soils commonly used in geotechnical engineering applications. Further, consideration of the role of compaction conditions (i.e., the soil structure associated with a given initial dry density and water content during compaction) on the thermal effects on capacitance sensors is needed to apply the measurements from these sensors to geotechnical projects. Current calibrations have been made primarily for agricultural applications where the soil is relatively loose (Evelt et al. 2002; Walker et al. 2004; Bogena et al. 2007; Assouline et al. 2010). Accordingly, this study focuses on the development of a correction equation for capacitance sensors to adjust for the impact of temperature changes and initial compaction conditions on the inferred values of volumetric water content.

1.2 Problem Statement

Capacitance sensors infer volumetric water content by measuring the apparent dielectric permittivity (referred to as the permittivity after this point for simplicity) of the soil. The permittivity of a soil is a function of the individual permittivity values of its constituents: soil particles, air and water. The permittivity is primarily influenced by volumetric water content (Davis and Annan 1976). In addition, measurements from capacitance sensors have been found to be sensitive to salinity, dry density, mineral/clay content, soil fabric, and temperature (Topp et al. 1980). Of these topics, the effects of temperature on capacitance sensors has not been thoroughly investigated. Most of the work that has been done to date on this topic has been to evaluate approaches to extract the impact of diurnal temperature changes on the response of dielectric sensors using multiple regression analyses or averaging (Assouline et al. 2010; Cobos et al. 2013). Past research on the effect of temperature on dielectric permittivity has found contradicting results. Some studies report either no temperature effects (Topp et al. 1980) or strong positive or negative correlation between temperature and permittivity (Wraith and Or

1999; Evett et al. 2006). This discrepancy in the observed trends implies that this topic deserves further study for different soils. Further, the coupled effects of initial conditions (i.e., initial volumetric water content and density of the soil) on the response of the dielectric sensor to heating are an important topic that would be useful to understand for thermally active geotechnical systems.

1.3 Objective

The objective of this study is to better understand the influence of temperature on the 5TM capacitance sensor from Decagon Devices of Pullman, Washington when used in a low-plasticity silt, and to develop a practical methodology that can be used to define thermal calibration equations to consider the role of initial gravimetric water content and dry density for this specific sensor. Throughout this paper, this sensor is referred to as a capacitance sensor, although it is capable of measuring both the temperature as well as inferring the dielectric permittivity. While it is generally accepted that changes in temperature affects the response of capacitance sensors, there are no generally accepted corrections for this type of soil. Although it is expected that the soil type may play an important role in the effects of temperature on the sensor response, only a single soil was investigated in this study, albeit under a range of compaction conditions. Using a low-plasticity silt helps to restrict the effects of temperature to the response of the soil itself as the effects of physico-chemical processes associated with charge imbalance on the soil particles (e.g., bonded water) are not expected during heating of the soil.

1.4 Approach

The experimental procedures involved heating a compacted layer of Bonny silt containing a dielectric sensor in a 60 °C oven. The goal of these tests was to keep the volumetric water content of the silt constant during the heating process so that the effects of temperature on the sensor response could be isolated. The column of Bonny silt was compacted within a sealed

mold and placed into the oven, after which transient changes in the sensor response were monitored. Before and after heating, the distribution in gravimetric water content was measured to observe any potential water migration effects. In addition to the temperature response of the sensors during heating, the correlation between the volumetric water content measured before heating and the dielectric permittivity as measured by the sensor allowed the development of a soil-specific calibration equation for Bonny silt at room temperature conditions.

In addition to several baseline tests intended to evaluate the impact of temperature on the sensor in water, air, and dry soil, three series of tests were performed as part of this study. The first series involved performing tests having the same initial conditions but with different durations of heating. These tests were useful to verify that the heating process does not lead to movement of water within the soil layer. The second and third series of tests involved changing the initial gravimetric water content for a constant dry density and changing the initial dry density for a constant gravimetric water content, respectively. Although a soil-specific calibration equation was developed as part of this study, the temperature effects were analyzed using the measured dielectric permittivity and not the calculated volumetric water contents.

1.5 Scope

This thesis is organized as follows: Chapter 2 provides a review of previous literature related to this topic, including a summary of water content measurement techniques and the electrical properties of soils. Chapter 3 presents the experimental setup and instrumentation utilized for this research. The material properties of the soil are presented in Chapter 4. The results obtained from testing are presented in Chapter 5. Chapter 6 describes the analysis that includes an evaluation of the impact of dry density on the calibration of the capacitance sensors at room temperature conditions, along with the development of a correction equation to consider the impact of temperature on the measured dielectric permittivity for different initial conditions.

CHAPTER 2

BACKGROUND AND LITERATURE REVIEW

2.1 Water Retention in Unsaturated Soils

2.1.1 Expressions for Water Content

Unsaturated soils are a three phase medium, consisting of air, water and soil particles. The soil matrix is comprised of mineral particles that play an important role in both soil behavior and classification. Water exists within the matrix in one of three phases: water vapor, free water (pore water) and bound water (adhered to the surface of soil particles). The bound and free pore water are subject to cohesive and adhesive forces that bind the water molecules to each other and to the surface of the soil particles. The amount of water in soils can be described using different terms that are derived from the phase diagram, as follows:

- Volumetric water content (θ_w or VWC) – the ratio of the volume of water to the total volume. This variable is commonly used in water flow applications. The maximum value of the volumetric water content occurs when the soil is saturated, in which case it is equal to the porosity (n). The porosity is equal to the ratio of the volume of voids to the total volume.
- Degree of saturation (S_r) – the percentage of the volume of voids that is occupied by soil water, equal to the volume of water divided by the volume of voids.
- Effective saturation (S_e) – a ratio similar to the degree of saturation, but normalized with respect to the residual saturation. This is equal to $(1 - S_r) / (S_r - S_{res})$, where S_{res} is the residual saturation. This term is commonly used in water retention models such as that of van Genuchten (1980).
- Gravimetric water content (w) – the ratio of the weight of water to the weight of dry soil particles. This variable is commonly used in compaction analyses. The gravimetric water content of soils can change regardless if a soil is saturated, and is related to the degree of

saturation through the void ratio (e), as follows: $w = Se/G_s$, where G_s is the specific gravity of the soil particles. The void ratio is the volume of voids divided by the volume of solids and is commonly used to infer soil volume changes because it is normalized by the volume of soils, which does not change during compression.

Because the dielectric permittivity of soils is determined through a sampling volume, the volumetric water content is used in calibration equations (Topp et al. 1980). However, the volumetric water content is not easy to measure directly. On the other hand, the gravimetric water content and total density of the soil are easier to determine. The gravimetric water content can be determined using oven drying (ASTM D2216-05) while the total density can be determined by measuring the total mass and volume of a soil specimen. Using these variables, the volumetric water content can be calculated as follows:

$$\theta_w = \frac{\rho_d}{\rho_w} w = \frac{\rho_t}{(1 - w)\rho_w} w \quad (2.1)$$

where ρ_t is the total density and ρ_d is the dry density.

2.1.2 Matric Suction and the Soil Water Retention Curve

In the absence of changes in air pressure, the pore water pressure above the water table is negative. The difference between the pore air pressure and the pore water pressure is known as matric suction. As the matric suction increases, the amount of water in the soil decreases. The storage of water in an unsaturated soil can be described using the soil water retention curve (SWRC), which is the relationship between the degree of saturation (or volumetric water content) and suction. Idealized SWRCs for different materials are shown in Figure 2.1.

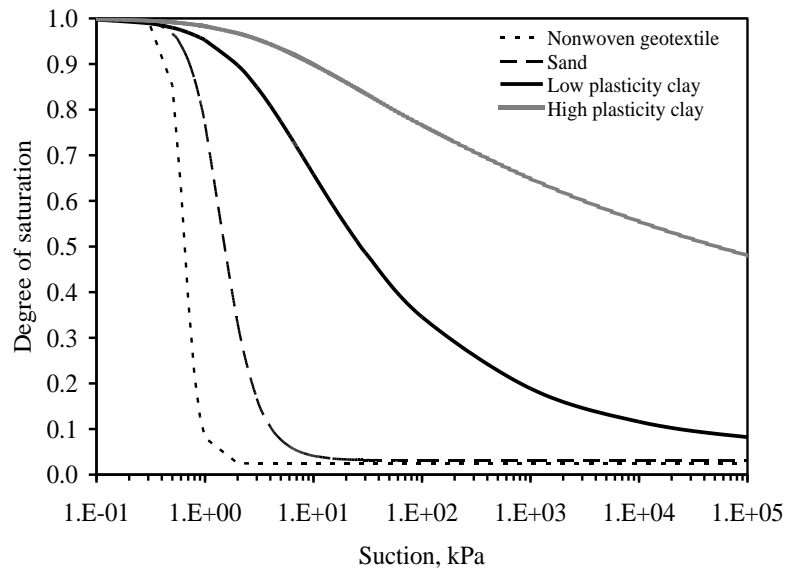


Figure 2.1 Drying-path SWRCs for different geotechnical materials (McCartney 2007)

The SWRC for a given soil decreases from a value of 1 at saturation to the residual saturation, a point where water only exists in bound form, adhered to the surface of the soil particles and can only be extracted in water vapor form. The SWRC curve is hysteric, which means that the curve follows different paths during drying and wetting. The range in suction over which a significant decrease in volumetric water content occurs is affected by the particle size distribution of the soil, as well as the soil mineralogy. As suction is often difficult to measure in the field, measurement of volumetric water content can be a very important alternative.

2.2 Electromagnetic Properties

2.2.1 Overview

The electromagnetic properties of soils are commonly measured to indirectly determine geotechnical properties such as dry density, water content, void ratio and anisotropy. The electromagnetic properties of interest are electrical conductivity, magnetic permeability, and dielectric permittivity (Liu 2007).

2.2.2 Electrical Conductivity

Electrical conductivity (σ) is a measure of a material's ability to conduct an electrical current. Soil particles typically exhibit relatively low electrical conductivity. However, pore water is comprised of water and ions; ions that are not electrically neutral. The electrical conductivity of a soil is predominately affected by its water content, then temperature and salt content. In clays, the high specific surface area causes an abundance of cations to build up in the pore fluid closest to the particle surface. This increases the electric conductivity along the surface of the clay particles and can have a significant impact on the overall electrical conductivity for clays with low degrees of saturation.

2.2.3 Magnetic Permeability

Magnetic permeability (μ) describes how much a material will magnetize during application of an external magnetic field. This property is most commonly applied to ferromagnetic materials like iron, cobalt and nickel, but it could be relevant in iron-rich residual soils. Most soils are either diamagnetic or paramagnetic (not natural magnets) and cannot support a magnetic field.

2.2.4 Dielectric Permittivity

The dielectric permittivity is a measure of the flux density generated by an electric field in a given material. It is commonly expressed as a "dielectric constant" which is the ratio of the absolute permittivity to the permittivity of a vacuum. While the permittivity of a vacuum is a constant ($\epsilon_0 = 8.85 \times 10^{-12}$ F/m), the permittivity of most materials is frequency dependent and therefore a complex number comprised of "real" and "imaginary" parts. The "real" part (ϵ') is related to the permittivity of the soil materials themselves (air, water and soil minerals). The "imaginary" part (ϵ'') is related to the dielectric losses, or the energy that is lost during application of an electromagnetic pulse, and the conduction of electricity within the material.

2.3 Water Content Sensors

2.3.1 Overview

There are various techniques, both destructive and non-destructive, for obtaining the volumetric water content of soil. Although oven-drying permits a simple and reliable approach to measure the gravimetric water content, this approach cannot be used easily to monitor transient changes in water content in soils. It is also not possible to characterize the coupled role of temperature changes, and the dry density of the soil must be known to relate the gravimetric water content to the volumetric water content. Gravimetric measurements are useful in calibrating non-destructive methods of water content determination that are described below.

2.3.2 Neutron Probe (NP)

The neutron probe emits radioactive particles at high velocities into the soil of interest. Particles experience a significant reduction in velocity upon collision with hydrogen particles. The probe measures the number of slow moving particles that return to the probe and correlates this to a soil moisture number. The neutron probe uses a large sampling volume, increasing the accuracy of its measurements. It does require a soil specific calibration but is insensitive to changes in temperature and electrical conductivity (Evetts et al. 2002)

2.3.3 Electrical Resistivity Probes

Electrical resistivity probes use the fact that water in soils is able to conduct electricity. In this case, the lower the amount of water in soils, the greater the resistance to current flow during application of an external electric field. This approach typically has the lowest resolution in measuring water content changes at a point, and is highly affected by variables like salinity.

2.3.4 Dielectric Sensors

Most nondestructive techniques to infer changes in volumetric water content actually infer changes in the dielectric permittivity of soil. The bulk dielectric permittivity of soils is considered a weighted average of the individual permittivity values of soil constituents (particles, water, and air). Water has a relatively high permittivity ($\epsilon = 80$ at 20°C) as compared to that of air ($\epsilon = 1$) and soil minerals. The value of permittivity for soil minerals ranges from 5 to 12, depending on mineralogy (Jones and Or 2002). Due to the high permittivity of water, small increases in volumetric water content significantly increase the average or apparent dielectric permittivity of the soil mixture.

2.3.3.1 Time Domain Reflectometry (TDR)

One type of electrical sensor uses Time Domain Reflectometry to measure the permittivity. TDR requires the installation of two to three parallel steel rods (wave guides) in the soil. An electric pulse is transmitted along the steel rods. The pulse is reflected at every change in impedance, including the beginning and end of the wave guides. The reflected waveform is interpreted to define the time travel of the electromagnetic wave through the wave guides, which is a function of the dielectric permittivity of the soil (Topp et al. 1980). For materials with high saturation levels or electrical conductivity values, signal loss of the wave form can occur creating difficulties in interpreting the return time.

2.3.3.2 Frequency Domain Reflectometry (FDR)

Frequency-domain sensors consist of two to three prongs that act as the plates of a capacitor with the soil acting as the dielectric material in between. A voltage step is applied to the capacitor, creating an oscillating electromagnetic wave through a circuit involving the soil. The frequency of the wave is a function of the dielectric permittivity of the soil and the amplitude of the wave is a function of its electrical conductivity. The accuracy of the sensor has been verified

by several studies though a decrease in accuracy emerge at extremely high or extremely low levels of saturation. The sampling volume of the sensor is limited to material within a few centimeters of the prongs. This increases the sensor's sensitivity to local irregularities caused by roots, gravel or voids (Baumhardt et al. 2000). These sensors include both capacitance sensors and electrical impedance sensors.

2.4 Variables that Affect Electromagnetic Measurements

2.4.1 Texture and Soil Fabric

Several secondary factors that affect the apparent dielectric permittivity of soils include the fabric associated with compaction conditions (i.e., wet or dry of the optimum water content), dry density, salinity and temperature

The results from experiments performed by Baumhardt and Lascano (2000) demonstrate that an increase in the soil water's salinity will increase the apparent volumetric water content as measured by a capacitance sensor. This was attributed to salinity effects on soil permittivity. Conflicting experiments have shown either an overestimation of water content due to increased salinity or no effect. Nadler et al. (1999) summarized 21 different experiments on a variety of soils to characterize the effects of salinity, water content, and compaction conditions. In addition 2 field tests were performed. No conclusive trend was observed. Czarnomski et al. (2005) observed the difference in measurements for natural and repacked (secondary soil structure removed) soils. It was noticed that the volumetric water content was under predicted in repacked soils but that the measured values fell within the 95% prediction interval associated with the manufacturer's calibration. Rothe et al. (1997) found that the installation of a sensor probe (TDR) increased the local density of the soil around the sensor, increasing the volumetric water content.

2.4.2 Operation Frequency

As mentioned earlier, two of the electromagnetic properties, dielectric permittivity and magnetic permeability are affected by the frequency of the electromagnetic wave that is imposed on the circuit by the sensor. As the wave oscillates, the ions in the electron cloud within the material is pushed out of equilibrium. This process is time dependent; therefore the polarization of the particles in either direction lags out of phase with the electromagnetic wave. At a resonance (or relaxation) frequency, the charge moves against the restoring force. Both dielectric permittivity and magnetic permeability have real and imaginary parts that capture the magnitude and phase of the electromagnetic wave. The real part corresponds to the zero-frequency value for each parameter while the imaginary part accounts for energy loss due to polarization and electrical conductivity. The equation for the complex dielectric permittivity that characterizes both the polarization effect and energy losses is given below:

$$\varepsilon = \varepsilon' - j\left(\varepsilon'' + \frac{\sigma_{dc}}{2\pi f \varepsilon_0}\right) \quad (2.2)$$

where ε' and ε'' are the real and imaginary components of the dielectric permittivity, σ_{dc} is the electrical conductivity in a direct current system, f is the frequency of the electromagnetic wave and ε_0 is the dielectric permittivity of a vacuum (Davis and Annan 1977).

When a system reaches its resonance frequency, the imaginary part approaches zero. As the frequency changes, the magnitude of the imaginary part also changes. Energy loss due to electrical conductivity dominates the imaginary part under frequencies of 100 MHz. Exceeding this frequency, the energy loss due to polarization affects the magnitude of the imaginary part. Polarization has little effect on molecules in a solid but can highly affect molecules in a fluid such as water. For materials with high specific surface area, this effect, termed dielectric dispersion, can be considerable in the measurement of the dielectric permittivity and a decrease in the apparent dielectric permittivity with an increase in frequency can be observed (Liu 2007)

2.4.3 Temperature

As temperature increases, the dielectric permittivity of water decreases, as shown in Figure 2.2, (Malmberg and Maryott 1956). It would logically follow that the soil's overall permittivity would also decrease with an increase in temperature. Theoretically, it is expected that a negative correlation would exist between dielectric permittivity and temperature. However the dielectric permittivity values of most soil minerals and air do not appreciably change with temperature (Assouline et al. 2010). Some experiments, such as those described by Wraith and Or (1999) and Czarnomski et al. (2005) indicate a negative correlation with temperature and dielectric permittivity. One suggested explanation for these trends is that each part of the complex dielectric permittivity has a different relationship with temperature. As temperature increases, the real part (ϵ') decreases while the complex part (ϵ'') increases. In some soils, the real part dominates the overall dielectric permittivity while in others the complex part dominates. (Cobos et al. 2013)

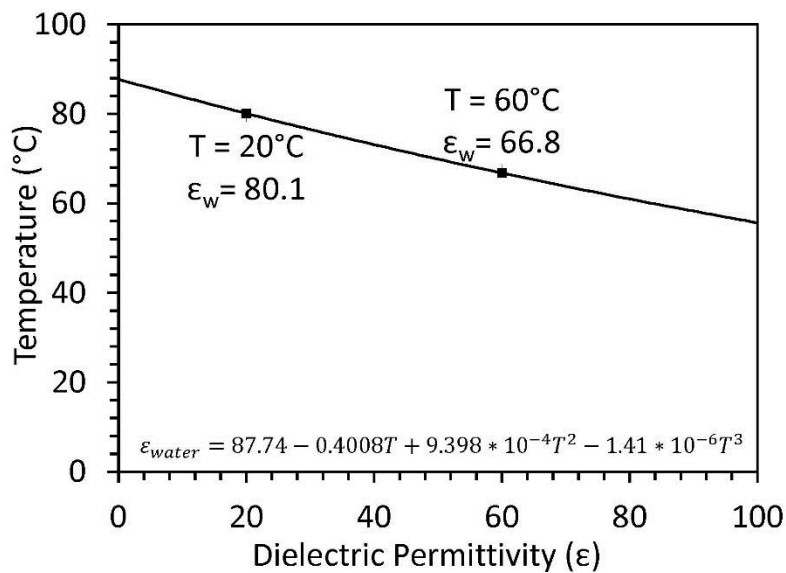


Figure 2.2: The dielectric permittivity of water as a function of temperature (Malmberg and Maryott 1956)

Many temperature dependence studies have used a large variety of soils at in-situ densities and water contents; however they did not consider intentionally placed and compacted soils for use in geotechnical applications rather than agricultural.

2.5 Previous Calibration Tests

Any dielectric technique requires a correlation to define the relationship between the measured value (time return for voltage pulse, electromagnetic wave frequency) and volumetric water content. Most involve a two-step calibration: first to relate the measured value to a dielectric permittivity and second to convert the dielectric permittivity to volumetric water content. A commonly used calibration equation is that of Topp et al. (1980), one of the first widely accepted dielectric permittivity to volumetric water content calibrations, given as follows:

$$\theta \text{ (m}^3\text{/m}^3\text{)} = 4.3 \times 10^{-6} \times \epsilon^3 - 5.5 \times 10^{-4} \times \epsilon^2 + 2.92 \times 10^{-2} \times \epsilon - 5.3 \times 10^{-2} \quad (2.2)$$

This equation was empirically developed using TDR technology. Although this equation provides a good estimate of the volumetric water content for low-plasticity soils, it does not consider the role of compaction conditions or temperature effects. Pozzato et al. (2007) presented a modification to Topp's equation to consider the role of dry density for silt.

The default factory calibration used by Decagon's software is based on this equation developed by Topp et al. (1980). Decagon recommends the development of a soil-specific calibration that will reduce error from 3-4% (in mineral soils, 10+% in high salinity or non-normal mineralogy soils) to 1-2%, increasing the accuracy of the capacitance sensors equal to that of the TDR system but with less capital cost. Following the experiments of Topp et al. (1980), Roth et al. (1990) developed a calibration based on a dielectric mixing model calibrated using TDR measurements in a variety of soils. Another mixing model was developed by Wraith and Or (1999) that focused on specific surface area as a major component of the dielectric permittivity of soil water. They noticed a variety of temperature effects: decreasing trends,

increasing trends and a combination of the two. They attributed these effects to the presence of bound water in the soil matrix and its transition to free water with the changes in temperature. Baumhardt et al. (2000) attempted to quantify diurnal VWC fluctuations recorded by EnviroSCAN capacitance sensor. They determined that the factory calibration was accurate for nearly dry soils but not for saturated samples. They also noticed temperature and salinity effects and attributed to changes in dielectric permittivity of the soil.

Czarnomski et al. (2006) performed experiments on two types of northwest-Pacific soils (a sandy loam and a gravelly clay loam) to compare the accuracy of three soil moisture sensors. The capacitance sensor was the only sensor to observe a temperature sensitivity. Evett et al. (2006) also reviewed three types of sensors to evaluate their accuracy, precision, and the benefits of soil-specific calibrations. They determined that the capacitance probes are highly sensitive to changes in electrical conductivity (above 10 ds/m) and tended to overestimate the water content in dry silty clays. They developed a temperature correction equation to remove the negative effects of temperature on volumetric water content. They observed the following relationship between volumetric water content and change in temperature, as follows:

$$\theta = 0.030 + 0.000938 \times \Delta T \quad (2.3)$$

In this equation, θ is the volumetric water content in percent and ΔT is the change in temperature in degrees Celsius.

CHAPTER 3

MATERIALS

3.1 Overview

This section presents the silt material used for the thermal experiments and its relevant geotechnical, hydraulic and thermal properties. The silt was recovered from the Bonny dam near the Colorado-Kansas border (referred to as Bonny silt). The soil has a low plasticity so changes in soil-pore water interactions as a result of temperature changes are not expected. This soil has been used in several recent studies focused on physical modeling of thermo-active geotechnical systems (Coccia and McCartney 2013; Stewart et al. 2014; Murphy and McCartney 2014). The silt in the tests was prepared using static compaction, which permits an unsaturated soil specimen to be formed with a uniform volumetric water content and dry density. An extensive database of laboratory test results on the mechanical and thermal properties of this soil is also available.

3.2 Geotechnical Characterization

3.2.1 Overview

Several tests were performed on Bonny silt so that it could be characterized using the Unified Soil Classification Scheme (USCS). The grain size distribution analysis was performed following ASTM D422. A hydrometer was used to determine the distribution of particles passing No. 200 sieve, while a sieve analysis was used to determine the distribution of particles retained on the No. 200 sieve. The grain size distribution is shown in Figure 3.1 and characteristic grain size values are presented in Table 3.1.

As Bonny silt has greater than 50% fines, the Atterberg limits were measured following ASTM D4318. The Atterberg limits for Bonny silt are presented in Table 3.2. Based on the grain size distribution data and the Atterberg limits, Bonny silt is classified as ML according to the USCS.

Table 3.1: Grain size distribution data for Bonny silt

| Parameter | Value |
|-------------------------|------------|
| D ₁₀ | <0.0013 mm |
| D ₃₀ | 0.022 mm |
| D ₅₀ | 0.039 mm |
| % Passing No. 200 Sieve | 83.9% |
| % Clay Size | 14.0% |
| % Silt Size | 69.9% |
| % Sand Size | 16.1% |

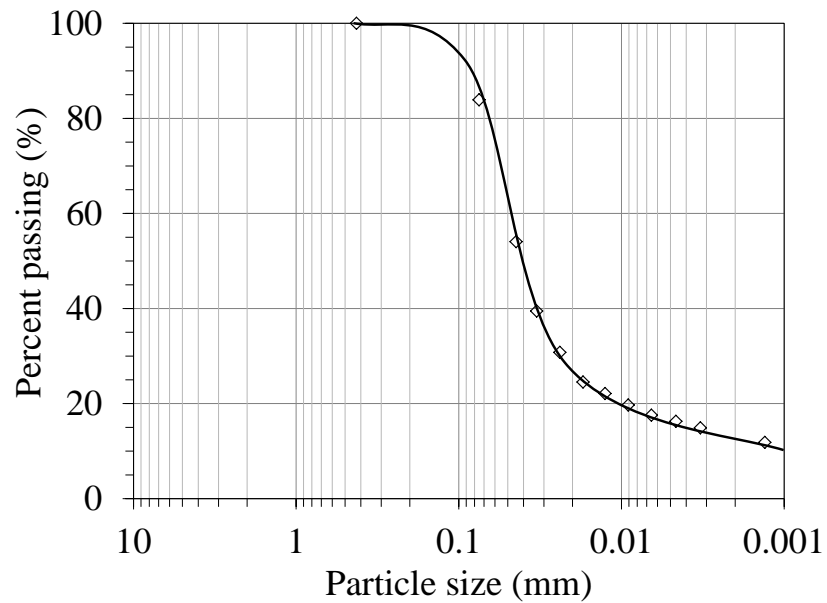


Figure 3.1: Grain size distribution curve for Bonny silt

Table 3.2: Atterberg limits for Bonny silt

| Parameter | Value |
|------------------|-------|
| Liquid limit | 24 |
| Plastic limit | 21 |
| Plasticity index | 4 |

The specific gravity of a soil (G_s) is defined as the ratio of a mass of a specific volume of the soil solids as compared with the mass of that same volume of water at 20°C. A value for G_s of

2.65 was used based on tests performed by El Tawati (2010). The compaction curves were obtained for the silt using both the standard (ASTM D698) and modified (ASTM D1557) compaction techniques. The compaction curves are presented in Figure 3.2. For the standard Proctor compaction effort, the optimum water content is 13.2% and the maximum dry density is 16.3 kN/m^3 . The zero air voids line was defined for $S_r = 1$ and $G_s = 2.65$.

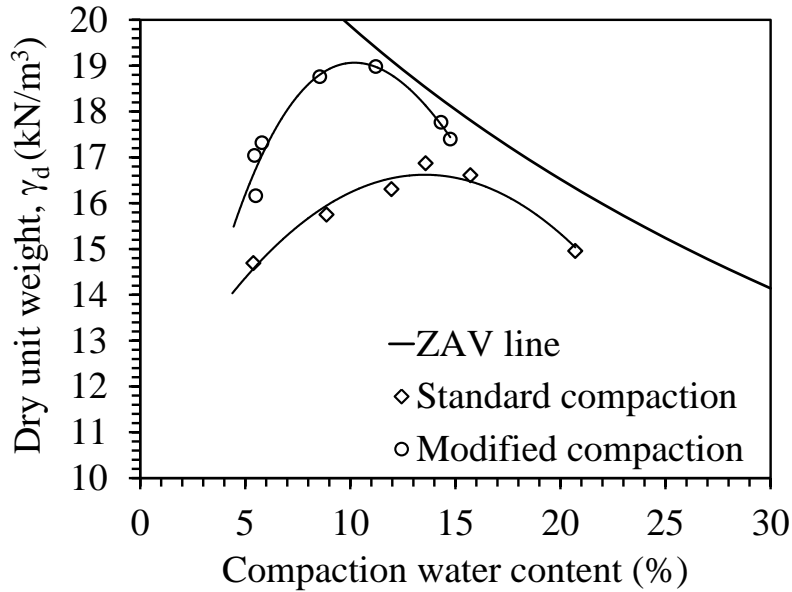


Figure 3.2: Compaction curves for Bonny silt obtained using both standard and modified Proctor compaction efforts, plotted with the zero air void (ZAV) line

3.2.2 Hydraulic Properties

The hydraulic properties of Bonny silt were measured using the flow pump technique developed by Aiban and Znidarčić (1989). This technique was used to define the saturated hydraulic conductivity using a constant flow rate approach, and was later combined with the axis-translation technique to measure the soil-water retention curve (SWRC) and hydraulic conductivity function (HCF) of unsaturated soils. A plot of saturated hydraulic conductivity for a variety of void ratios is presented in Figure 3.3. The data for this plot was taken from previous

literature published using this technique. The hydraulic conductivity of saturated specimens having initial void ratios ranging from 0.5 to 0.8 ranges from 1×10^{-9} to 1×10^{-7} m/s.

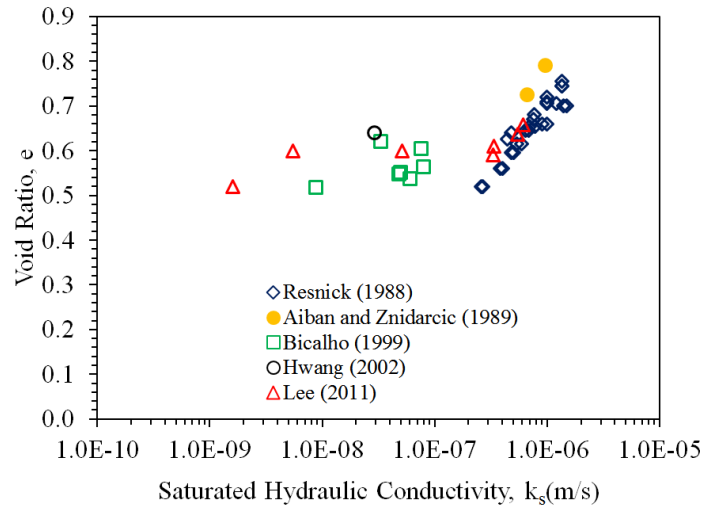


Figure 3.3: Hydraulic conductivity as a function of void ratio for Bonny silt

The SWRCs for Bonny silt specimens having an initial void ratio of 0.69 under a range of net stresses are shown in Figure 3.4. These SWRC curves were defined by first saturating compacted specimens then draining them using a flow pump. This approach only permitted drainage of water up to a suction of 70 kPa before no further water could be withdrawn. The curves emphasize the importance of effective stress state and the initial pore size distribution of the soil on the hydraulic properties.

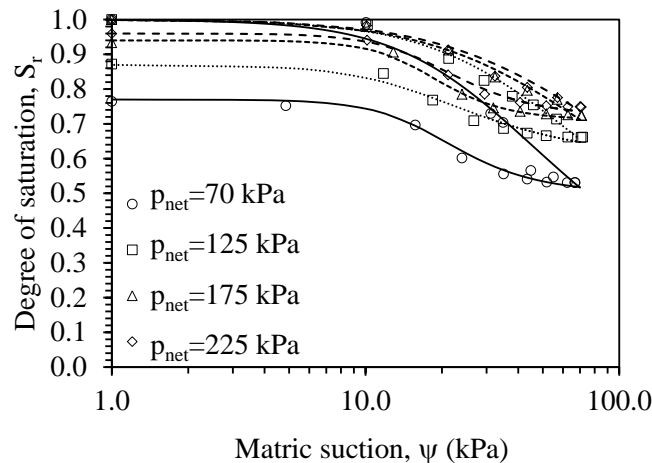


Figure 3.4: SWRCs for Bonny silt specimens having an initial void ratio of 0.69 under a range of net stresses (Khosravi 2012)

3.2.3 Thermal Properties

The thermal conductivity of Bonny silt as a function of void ratio was obtained using a triaxial cell adapted to accommodate a miniature thermal needle (70 mm length) probe in the top platen. The needle probe was used to infer the thermal conductivity of the soil specimen using the line-source equation. The thermal conductivity of Bonny silt was measured after isotropic consolidation of a cylindrical specimen to different void ratios, with typical results from two tests shown in Figure 3.5.

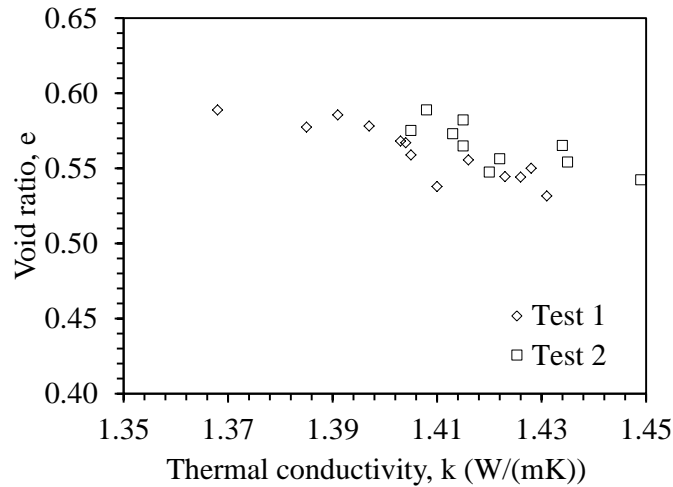


Figure 3.5: Relationship between thermal conductivity and void ratio for Bonny silt

CHAPTER 4

EXPERIMENTAL SETUP AND APPROACH

4.1 Overview

A testing methodology was developed to evaluate the impact of changes in temperature on the response of a capacitance sensor in a layer of soil under undrained (constant water content) conditions. Changes in temperature may affect the apparent dielectric permittivity measurements from a capacitance sensor that is monitoring water flow processes, correlating to an incorrect volumetric water content value and a false indication of change in water content. Accordingly, the goal of the tests was to encapsulate a compacted soil specimen such that changes in water content during heating will not occur, so that only temperature effects on the sensor will be observed.

4.2 Compaction Mold

The experiments were performed on soil layers that were compacted within a 152 mm-diameter modified Proctor mold. The base plate and extension collar were constructed of steel and conform to specifications in ASTM D698. The mold itself is a 178 mm-tall section of PVC pipe, identical in inside dimensions of a modified Proctor mold. The reason for using PVC is to avoid any electrical interference between the mold and the dielectric sensor. A 17 mm-diameter hole was drilled into the wall of the mold to allow the cable for the dielectric sensor to exit. The sides of the mold are assumed to be impermeable, but one of the goals of this experiment was to avoid any loss of water from the compacted soil layer during heating. Accordingly, four layers of low-density polyethylene sheeting (Saran Wrap) were sandwiched between the bottom of the mold and the side wall, and between the top of the soil layer and the collar. During compaction, a capacitance sensor was embedded within the soil layer during compaction. Schematics of the

mold are shown in Figure 4.1 which highlights the dimensions, the location of the sensor and the zone of influence, approximately 300 cm^3 around the sensor (Decagon Devices 2014).

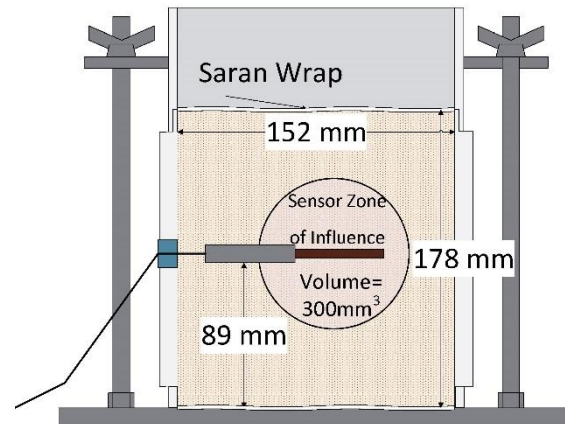


Figure 4.1 Schematic of the compaction mold used for all experiments. Shows rubber stopper plug used to seal sensor wire exiting mold and the location of the sensor (and its zone of influence) after compaction.

4.3 Instrumentation

The capacitance sensor evaluated in this study is 5TM® dielectric sensor manufactured by Decagon Devices. This sensor measures the dielectric permittivity via its three prongs embedded in the soil which together form a capacitor circuit, as well as the temperature via a thermistor mounted on the base, in direct contact with the soil. The thermistor is capable of measuring changes in temperature from -40 to $60 \text{ }^\circ\text{C}$. The sensor is connected to an ECH20 EM50 data logger manufactured by Decagon Devices and data is collected using the ECH20 Utility Software.

The 5TM sensor measures the apparent dielectric permittivity of soil by imposing a 70 MHz oscillating electromagnetic wave through its prongs. Acting as a capacitor, the prongs build up a charge, proportional to the dielectric permittivity of the soil between the prongs. The sensor measures the charge time of the capacitor circuit, which is related to the bulk dielectric permittivity of the soil within the prongs. According to the manufacturer, the accuracy of the

sensor is $\pm 1 \epsilon_a$ for permittivity values ranging from 1 to 40 and $\pm 40 \epsilon_a$ for permittivity values exceeding 40 (Decagon Devices 2014). The sensor measures the bulk permittivity of soil, ranging from 1, which is representative of that of air (ϵ_{air}), to 80, which is representative of that of water (ϵ_{water}).

4.4 Soil Layer Preparation

The Bonny silt was prepared in large batches so that multiple specimens could be tested with similar water content. The soil was moisture-conditioned to a target gravimetric water content by misting water with a pressurized spray bottle while hand mixing. After adding a calculated amount of water to oven-dried soil, the moist soil was sealed in a plastic bucket for a minimum of 24 hours for equilibration. Prior to each test, samples were obtained to determine the actual water content of each soil sample using oven-drying. The gravimetric water content was used to calculate the dry density achieved during compaction, as mass and volume are easily measured to determine total density.

The soil was statically compacted into the mold in six lifts using a mechanical press, with each lift height marked on the inside of the mold. Scarification was performed between lifts to ensure good lift interface contact and minimize the formation of weak zones within the soil layer. The sensor was placed in between the third and fourth lifts in the center of the mold. Loose soil was placed above the intended height of the dielectric sensor, and the sensor was covered with more soil before this lift was compacted. The latter technique was done to provide some cushion for the dielectric sensor during compaction and to avoid damage. A sample compaction schedule is shown in Table 4.1. The experiments have been plotted with the standard and modified Proctor compaction curves for Bonny Silt, shown in Figure 4.2.

Table 4.1: Sample compaction details for the 3-hour test #1

| Lift | Mass (g) | Height (mm) | Total Density (kg/m ³) | Water Content (%) | Dry Density (kg/m ³) |
|----------|----------|-------------|------------------------------------|-------------------|----------------------------------|
| 1 | 825 | 29 | 1630 | 16.3 | 1400 |
| 2 | 822 | 29 | 1630 | 16.4 | 1400 |
| 3 | 826 | 29 | 1630 | 16.5 | 1400 |
| 4 | 818 | 29 | 1620 | 16.0 | 1390 |
| 5 | 823 | 29 | 1630 | 16.3 | 1400 |
| 6 | 815 | 29 | 1610 | 16.2 | 1390 |
| Average: | | | 1620 | | 1400 |

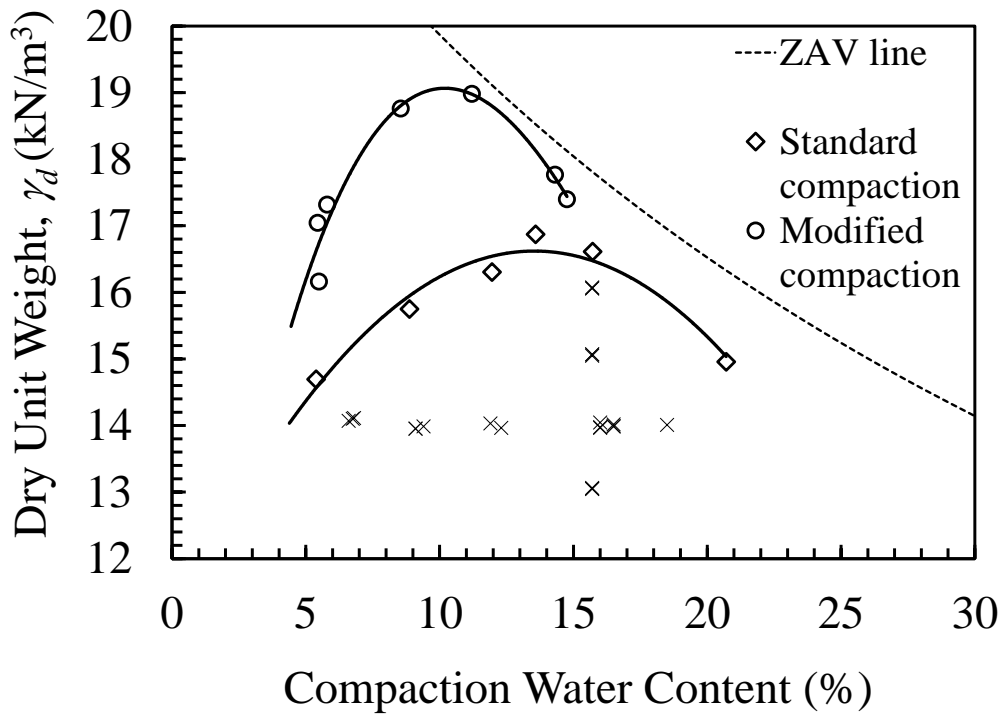


Figure 4.2: The initial conditions of all tests plotted over the Proctor curves for Bonny silt

CHAPTER 5

EXPERIMENTAL RESULTS

5.1 Overview

Several series of tests were performed to characterize the impact of temperature on the dielectric sensor. First, baseline tests were performed to evaluate the response of the sensor to changes in temperature in air and water, and in saturated and dry, compacted Bonny silt. Next, three series of tests were performed to evaluate the effects of changes in temperature, initial dry density and initial volumetric water content on the response of the dielectric sensor. Each test with a different condition was performed three times to evaluate variability in the sensor response and the initial conditions in the compacted soil layer. All tests were performed in a standard soil-drying oven using forced dry air with a temperature control. The oven was maintained at a constant temperature of 60°C. For all of the time series, data collection started (i.e., a time of zero) when the experimental mold was placed in the oven and was stopped when it was removed from the oven.

5.2 Baseline Test Results

First the sensor readings at $\theta_w = 0\%$ (air) and $\theta_w = 100\%$ (water) were confirmed to ensure the sensor was in proper working condition. The sensor recorded measurements while held in air and then again while in a container of room temperature water. These measurements corresponded to the minimum value for air (1) and maximum value for water (4094) that can be measured by the sensor. Next the sensor was placed in the oven to observe the temperature response on the sensor and the permittivity of the air in the oven, shown in Figure 5.1. This test demonstrates the sensor's response to changes in air temperature, showing if the sensor itself is sensitive to temperature changes. The sensor was heated for 1 hour and showed a slight increase in measured permittivity with increasing temperature. Despite this slight increase, these results

corroborate Decagon's statement that the sensor itself is "perfectly insensitive" to temperature effects (Cobos and Campbell 2013).

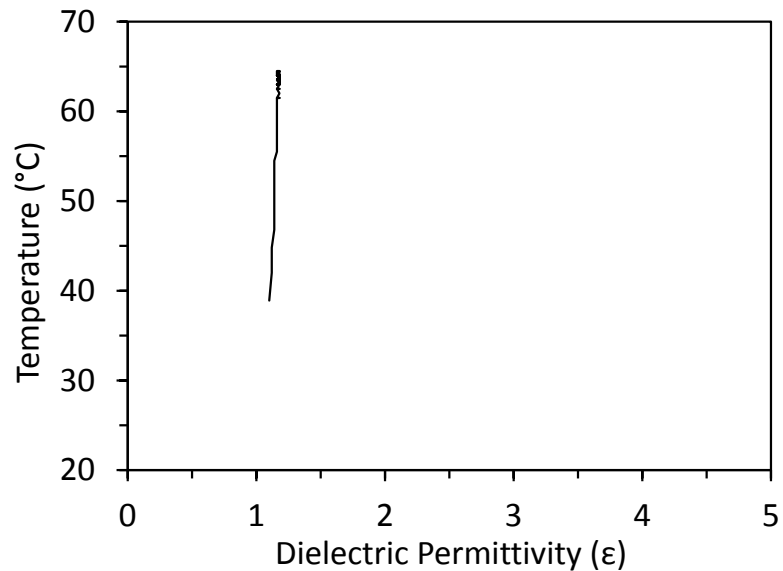


Figure 5.1: Results from the baseline test on a sensor in air plotted as the measured temperature versus the apparent dielectric permittivity

The final baseline test involved measurement of the sensor's response in dry and saturated soil samples. The dry soil was prepared by placing a volume of soil in a soil-drying oven for 48 hours then compacting it to a dry density of 1400 kg/m^3 . The saturated sample was prepared by submerging Bonny silt in water for 48 hours then densifying the wet soil in the mold by shaking the mold, achieving a dry density of 1455 kg/m^3 . The two specimens were heated for three hours. These tests established the bounds of expected thermal response in the Bonny silt at this dry density, as shown in Figure 5.2. In Figure 5.3, the temperature increase is plotted against the measured dielectric permittivity. The oven dried sample (VWC=0%) shows a 1% increase in apparent permittivity for the change in temperature of $25 \text{ }^\circ\text{C}$. The saturated soil specimen (VWC=50%) shows a 34% increase in apparent permittivity with increasing temperature during the test. These tests indicate that the presence of water has a significant impact on the temperature effect of the capacitance sensor.

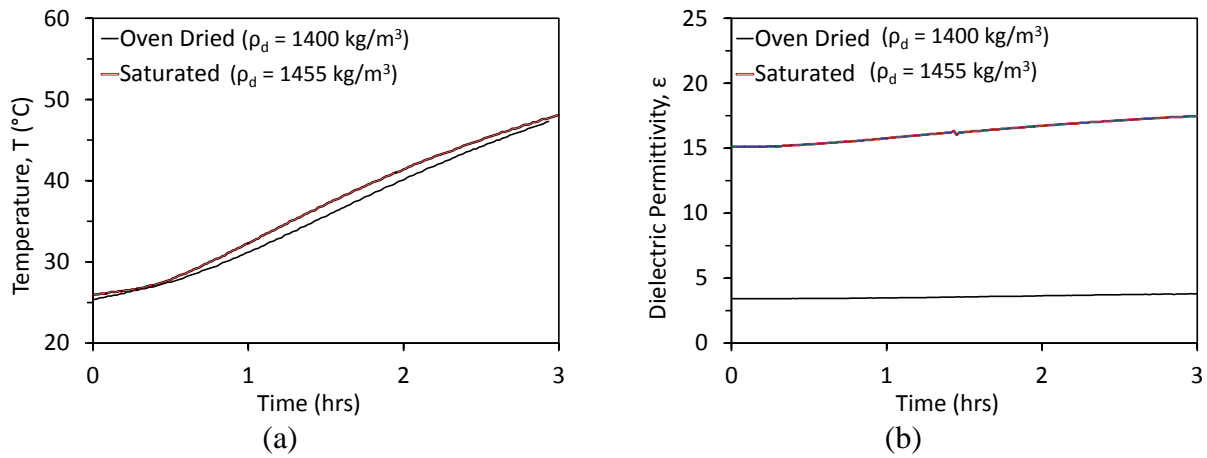


Figure 5.2: The time series data from the baseline tests showing the sensor response in a fully dry and fully saturated sample to a) temperature and b) dielectric permittivity.

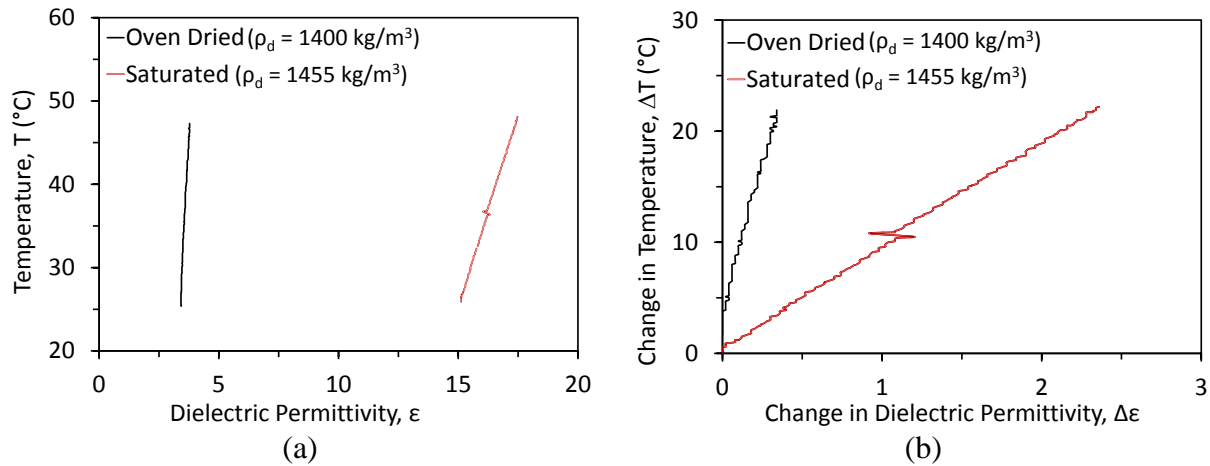


Figure 5.3: The baseline test results showing the changes in temperature as a function of dielectric permittivity. In (b) there is an initial increase in temperature but no change in dielectric permittivity, resulting in lines that do not originate at zero.

5.3 Evaluation of the Impact of Heating Duration Test Results

5.3.1 Overview

A summary of initial testing conditions for the tests performed to evaluate the impact of changes in temperature are summarized in Table 5.1. In these tests, the initial conditions (dry density, volumetric water content, void ratio, and saturation level.) were kept within 3% of each other on each of the repeated trials (T1 to T3). The reason that these tests were performed was to

evaluate whether heating the soil specimen for different amounts of time would lead to a change in the distribution of volumetric water content within the specimen.

Table 5.1: Compaction details for tests with varying duration of heating

| Test number | Specimen details | | | | | Testing |
|-------------|----------------------|-----------------------------------|------------|----------|----------------------|--------------|
| | Dry density | Volumetric water content | Void ratio | Porosity | Degree of saturation | Heating time |
| | (kg/m ³) | (m ³ /m ³) | | | | (hrs.) |
| T1-1 | 1399 | 0.23 | 0.89 | 0.47 | 0.49 | 1 |
| T1-2 | 1401 | 0.23 | 0.89 | 0.47 | 0.49 | 1 |
| T1-3 | 1402 | 0.23 | 0.89 | 0.47 | 0.49 | 1 |
| T2-1 | 1393 | 0.23 | 0.90 | 0.47 | 0.48 | 3 |
| T2-2 | 1402 | 0.23 | 0.89 | 0.47 | 0.49 | 3 |
| T2-3 | 1398 | 0.23 | 0.90 | 0.47 | 0.49 | 3 |
| T3-1 | 1395 | 0.22 | 0.90 | 0.47 | 0.47 | 5 |
| T3-2 | 1392 | 0.23 | 0.90 | 0.47 | 0.48 | 5 |
| T3-3 | 1400 | 0.23 | 0.89 | 0.47 | 0.49 | 5 |
| T4-1 | 1394 | 0.23 | 0.90 | 0.47 | 0.48 | 7 |
| T4-2 | 1397 | 0.23 | 0.90 | 0.47 | 0.49 | 7 |
| T4-3 | 1399 | 0.23 | 0.89 | 0.47 | 0.49 | 7 |

5.3.2 Time Series Data

The time series data of temperature and measured dielectric permittivity are shown in Figure 5.4. The results showed the expected increase in temperature and a rise in apparent dielectric permittivity. The trends appear to be similar regardless of heating duration. The heating duration did not lead to significant changes in results from 1 to 7 hours, except that the range of temperature changes experienced by the sensor changed. Accordingly, in order to obtain a reasonable change in temperature in each test all subsequent tests were heated for three hours.

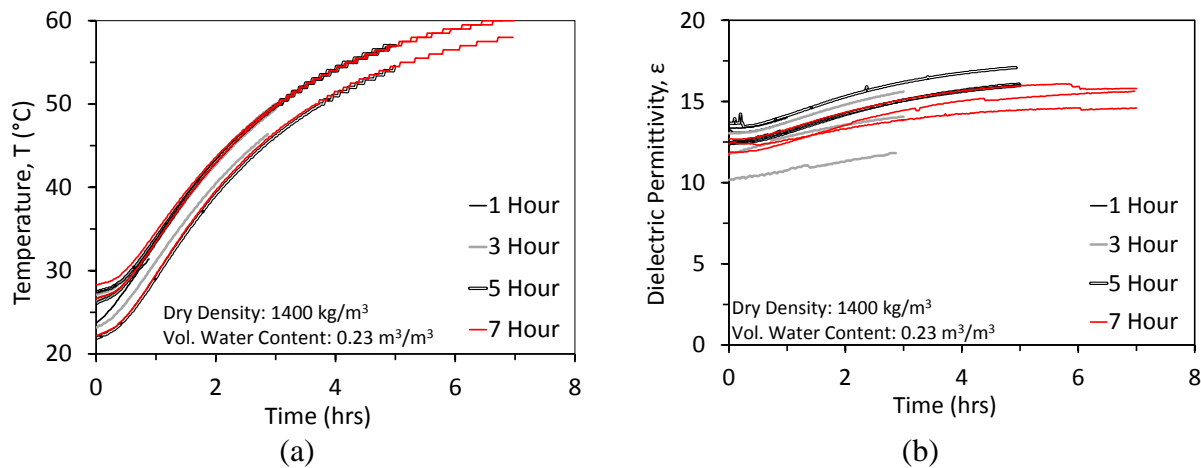


Figure 5.4: The time series data from the tests evaluating heating duration showing the sensor response to a) temperature and b) dielectric permittivity.

5.3.3 Water Content Profiles Before and After Heating

To ensure any measured changes in dielectric permittivity are directly related to temperature effects and not thermally induced water migration, gravimetric water content samples were taken after heating and compared to the initial gravimetric samples. Samples were taken from each lift; after heating, samples were taken from the edge of the mold and the center of the mold, to observe vertical and horizontal water migration. Locations from which the samples were taken are shown in Figure 5.5. The distributions in gravimetric water content with height in the different specimens heated for different durations are shown Figure 5.6. These results imply that the water content did not change significantly in the tests before and after heating, regardless of the time of heating. Not only do these results verify that the approach of using Saran wrap to encapsulate the soil layer is sufficient to minimize the loss of water from the soil, but also that the water content did not change with depth in the soil layer during heating. If the specimen were heated for a very long time, it is expected that water vapor would rise to the top of the soil layer due to buoyancy.

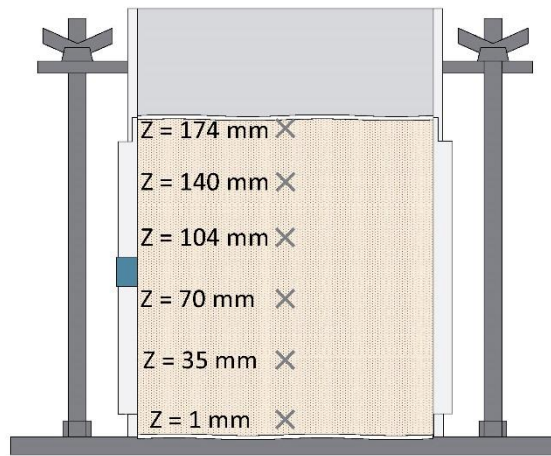


Figure 5.5: Location of gravimetric water content samples taken to check water migration

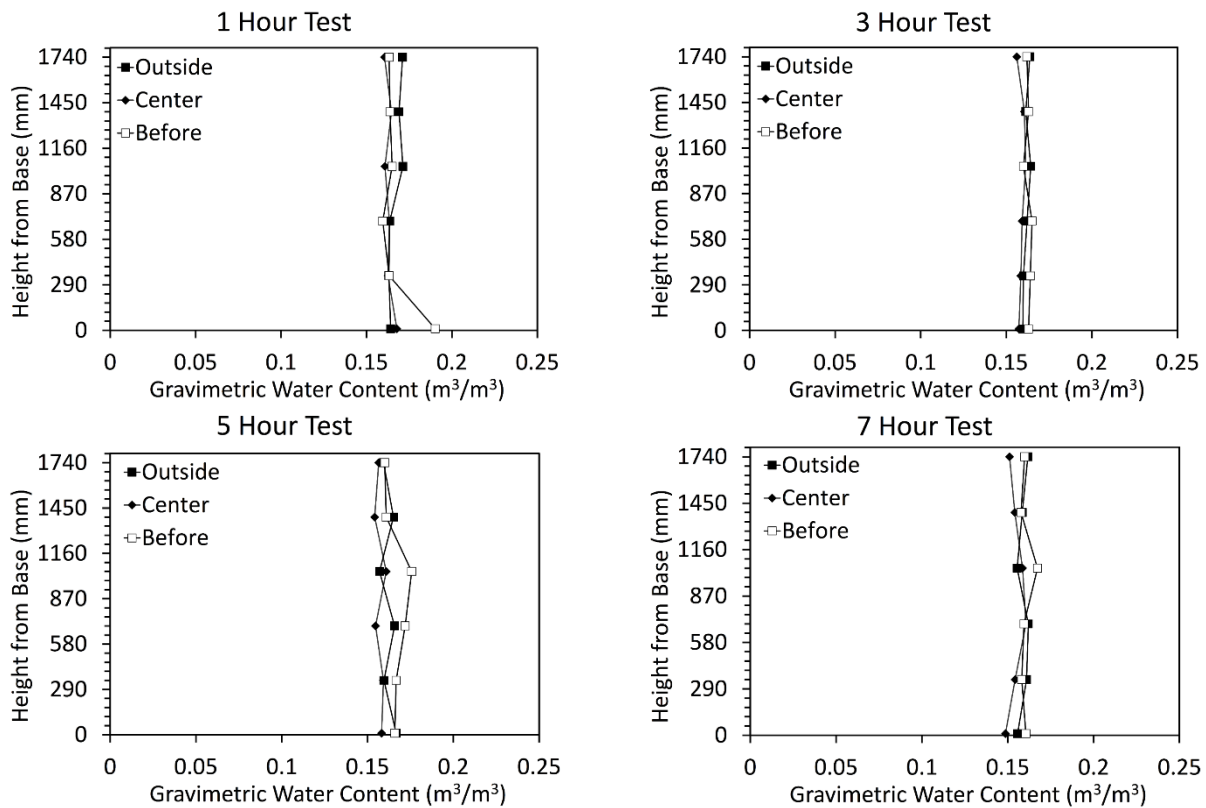


Figure 5.6: Profiles of gravimetric water content samples taken from each lift during compaction and after heating for different durations

The volumetric water content values obtained from Equation 2.1 before heating were then plotted against the values estimated by the data logger using Topp's Equation. Although the actual volumetric water content values were all consistent with each other, the initial values of

volumetric water content from Topp's equation do not fall onto the 1:1 line, shown in Figure 5.7. These results indicate that Topp's equation may not provide a good calibration for this soil. Accordingly, the results from this study were sufficient to define a soil-specific calibration that will improve the accuracy of the dielectric permittivity to volumetric water content conversion, which will be discussed further in Chapter 6. Further, the final water content values inferred by the sensor show a large increase compared to the initial sensor readings.

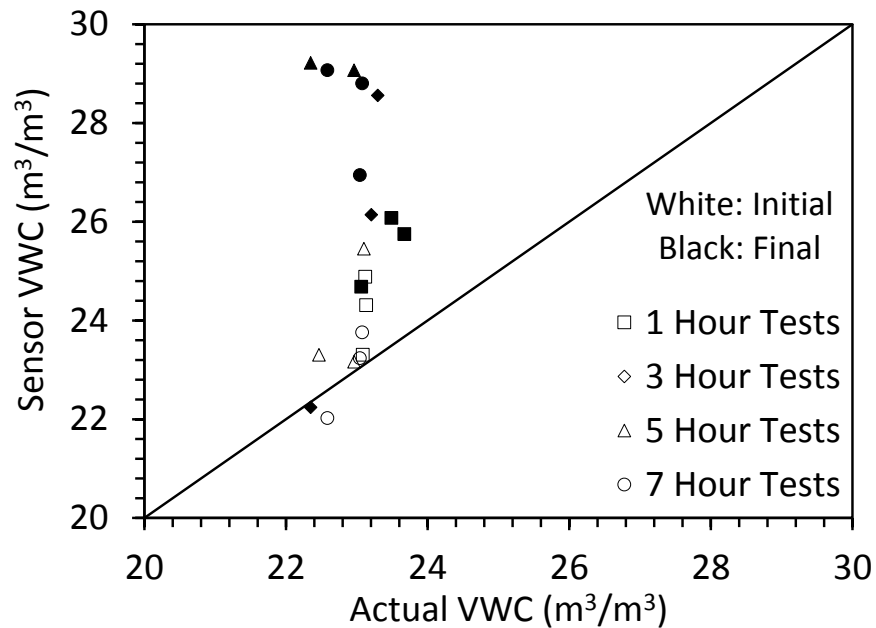


Figure 5.7: Plot of the calculated volumetric water content values versus the volumetric water content values inferred by the sensor using Topp's equation.

5.4 Evaluation of the Impact of Initial Water Content

5.4.1 Overview

A summary of initial testing conditions for the tests performed to evaluate the impact of the initial volumetric water content on the response of the sensor is shown in Table 5.2. The purpose of performing these tests is to understand if the dielectric sensor will infer a greater change in water content in a dryer soil due to vaporization of water during heating. It is possible that vaporized water could condense on the sensor and change the reading.

Table 5.2: Compaction details for tests with varying initial water contents

| Test number | Specimen details | | | | | | Testing details |
|-------------|----------------------|------------|----------|----------------------|-----------------------------------|-----------------------------------|-----------------|
| | Dry density | Void ratio | Porosity | Degree of saturation | Volumetric water content | Average vol. water | Heating time |
| | (kg/m ³) | | | | (m ³ /m ³) | (m ³ /m ³) | (hrs.) |
| WC1-1 | 1407 | 0.767 | 0.43 | 0.23 | 0.10 | 0.10 | 3 |
| WC1-2 | 1410 | 0.760 | 0.43 | 0.24 | 0.10 | | 3 |
| WC1-3 | 1411 | 0.758 | 0.43 | 0.24 | 0.10 | | 3 |
| WC2-1 | 1399 | 0.732 | 0.42 | 0.34 | 0.14 | 0.14 | 3 |
| WC2-2 | 1395 | 0.741 | 0.43 | 0.33 | 0.14 | | 3 |
| WC2-3 | 1395 | 0.741 | 0.43 | 0.33 | 0.14 | | 3 |
| WC3-1 | 1403 | 0.688 | 0.41 | 0.46 | 0.19 | 0.19 | 3 |
| WC3-2 | 1396 | 0.690 | 0.41 | 0.47 | 0.19 | | 3 |
| WC3-3 | 1400 | 0.686 | 0.41 | 0.48 | 0.19 | | 3 |
| WC4-1 | 1399 | 0.626 | 0.38 | 0.70 | 0.27 | 0.27 | 3 |
| WC4-2 | 1402 | 0.623 | 0.38 | 0.70 | 0.27 | | 3 |
| WC4-3 | 1398 | 0.627 | 0.39 | 0.70 | 0.27 | | 3 |
| WC5-1 | 1401 | 0.596 | 0.37 | 0.82 | 0.31 | 0.31 | 3 |

5.4.2 Time Series Data

Figure 5.8 shows the time series data for the tests varying initial water content. All tests experienced similar increases in temperature and measured dielectric permittivity. It is difficult to determine if the initial water content has any effect on the rate of increase in measured dielectric permittivity with the change in temperature.

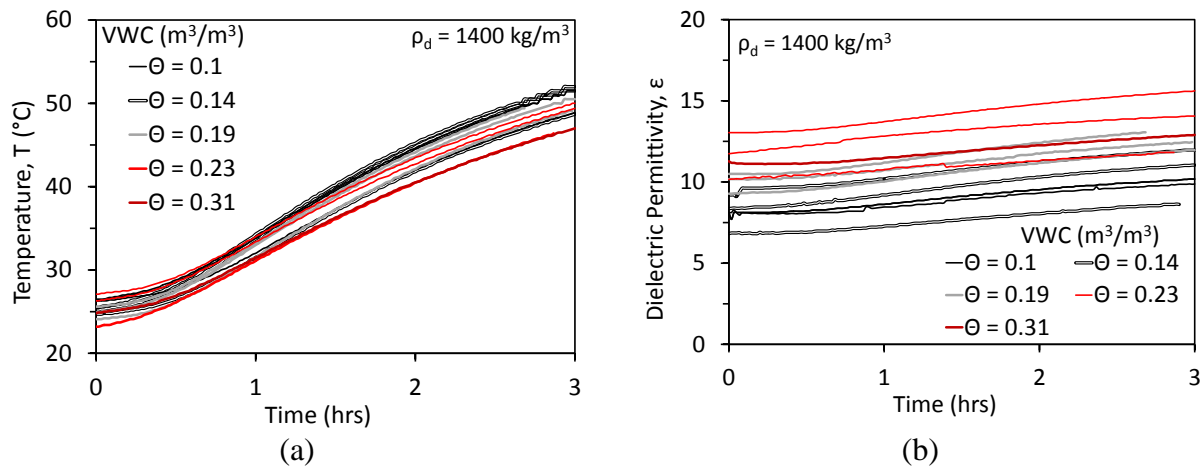


Figure 5.8: Effect of initial water content on the time series data of the a) temperature and b)

apparent dielectric permittivity

5.5 Evaluation of the Impact of Initial Dry Density

5.5.1 Overview

The last series of tests were performed on specimens having the same initial gravimetric water content as in the tests evaluating the impact of heating duration, but with varying initial dry density. As the sample dry density increases while the gravimetric water content remains constant, the volumetric water content also increases. Nonetheless, the initial volumetric water content values, which ranged from 0.22 to 0.25, are within 20% of each other. A summary of initial testing conditions for the tests performed to evaluate the impact of the initial dry density on the response of the sensor is shown in Table 5.3. Similar to the tests with the same initial volumetric water content, the heating duration was 3 hours. As geotechnical applications typically involve compacted soils, the role of different initial densities is important to evaluate.

Table 5.3: Compaction details for tests with varying initial dry densities.

| Test number | Specimen details | | | | | Testing details |
|-------------|----------------------|-----------------------------------|------------|----------|----------------------|-----------------|
| | Dry density | Volumetric water content | Void ratio | Porosity | Degree of saturation | Heating time |
| | (kg/m ³) | (m ³ /m ³) | | | | (hrs.) |
| D1-1 | 1305 | 0.20 | 1.03 | 0.51 | 0.40 | 3 |
| D1-2 | 1305 | 0.20 | 1.03 | 0.51 | 0.40 | 3 |
| D1-3 | 1306 | 0.21 | 1.03 | 0.51 | 0.40 | 3 |
| D2-1 | 1397 | 0.22 | 0.90 | 0.47 | 0.47 | 3 |
| D2-2 | 1398 | 0.22 | 0.90 | 0.47 | 0.47 | 3 |
| D2-3 | 1405 | 0.22 | 0.89 | 0.47 | 0.48 | 3 |
| D3-1 | 1507 | 0.24 | 0.76 | 0.43 | 0.55 | 3 |
| D3-2 | 1505 | 0.24 | 0.76 | 0.43 | 0.55 | 3 |
| D3-3 | 1507 | 0.24 | 0.76 | 0.43 | 0.55 | 3 |
| D4-1 | 1606 | 0.25 | 0.65 | 0.39 | 0.64 | 3 |
| D4-2 | 1606 | 0.25 | 0.65 | 0.39 | 0.64 | 3 |
| D4-3 | 1608 | 0.25 | 0.65 | 0.39 | 0.64 | 3 |

5.5.2 Time Series Data

Figure 5.9 shows the time series data for the tests that have different initial dry densities. All tests experienced similar increases in temperature. The increase in apparent dielectric permittivity appears to vary slightly with dry density.

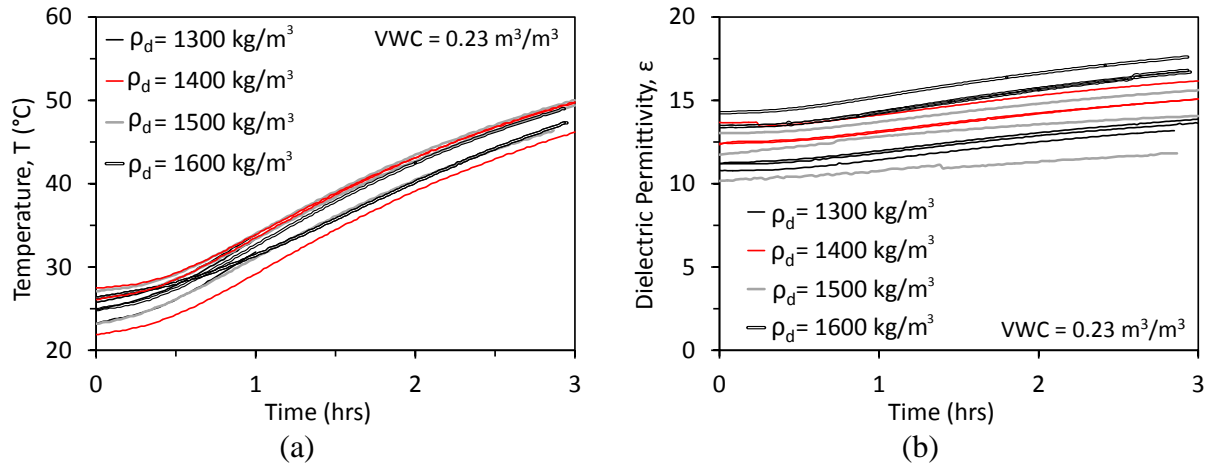


Figure 5.9: Effect of initial dry density on the time series data for: (a) Temperature; (b) Apparent dielectric permittivity.

CHAPTER 6

ANALYSIS

6.1 Overview

The data from the different test series were analyzed first to characterize the calibration curve for the capacitance sensors in Bonny silt at ambient temperature conditions. These tests are sufficient to consider the role of compaction conditions on the calibration curve. Next, the data from the second and third test series were analyzed to develop a correction equation for temperature effects on the capacitance sensor. This equation is used to account for the impact of the initial conditions (dry density and volumetric water content) on the slope of the relationship between the apparent dielectric permittivity and change in temperature measured in these tests.

6.2 Ambient Temperature Calibration

A soil-specific calibration was developed using the volumetric water content values calculated from the measured values of gravimetric water content and dry density and the initial readings of the capacitance sensor before heating. The data reported in sections 5.4 and 5.5 were used to develop this calibration. The apparent dielectric permittivity measurements and their corresponding volumetric water content values were plotted against each other, as shown in Figure 6.1. The data in this figure is separated by the initial dry density values of 1300, 1400, and 1600 kg/m³. Although there is some scatter in the data, the data follows a linear trend. Accordingly, the following form for the calibration equation was selected:

$$\theta = A\varepsilon + B \quad (6.1)$$

A linear trend was fit to the data at each different dry density. Each linear trend line was forced to intercept the abscissa at an approximate value for the dielectric permittivity of the dry Bonny silt specimens measured from the oven dried tests (3.34). Even with zero volumetric water content, the compacted soil particles will have a non-zero dielectric permittivity. In order to force

the trend lines to have a value of 3.34 at zero volumetric water content, the intercept on the ordinate axis had to be varied slightly from -0.09 to -0.11 m³/m³. An average intercept value of 0.1 m³/m³ can be used for the “B” factor in Equation 6.1. For comparison, Topp’s equation is also plotted in Figure 6.1. Although this equation provides a good fit to the data at volumetric water content values ranging from 0.1 to 0.25 m³/m³, it does not provide as good of a fit at low or high water contents. Topp’s equation shows nonlinear behavior at higher permittivity values due to the polynomial form of this equation.

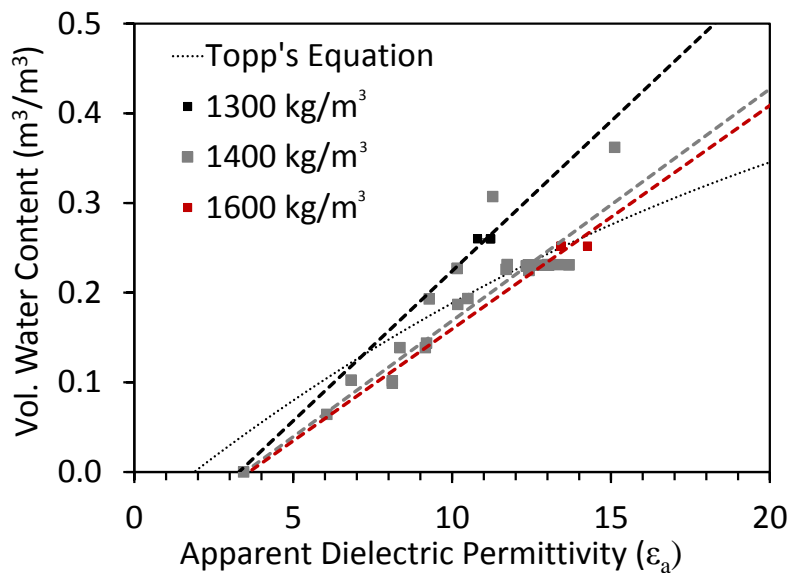


Figure 6.1: Soil specific calibration curves developed for measuring dielectric permittivity of Bonny silt at different initial dry densities using a capacitance sensor.

In Figure 6.1, a decreasing trend in the slope of the regression lines is observed in the groups of data with increasing dry density. The slopes of these lines are plotted in Figure 6.2, which indicate a linear decreasing trend between the slope (i.e., the “A” factor) and the dry density of the Bonny silt specimens. The calibration equation for Bonny silt considering the effect of density can be obtained by inserting the best-fit equation from Figure 6.2 into Equation 6.1, as follows:

$$\theta = (-2 * 10^{-5} \rho_d + 0.06)\varepsilon - 0.06 \quad (6.2)$$

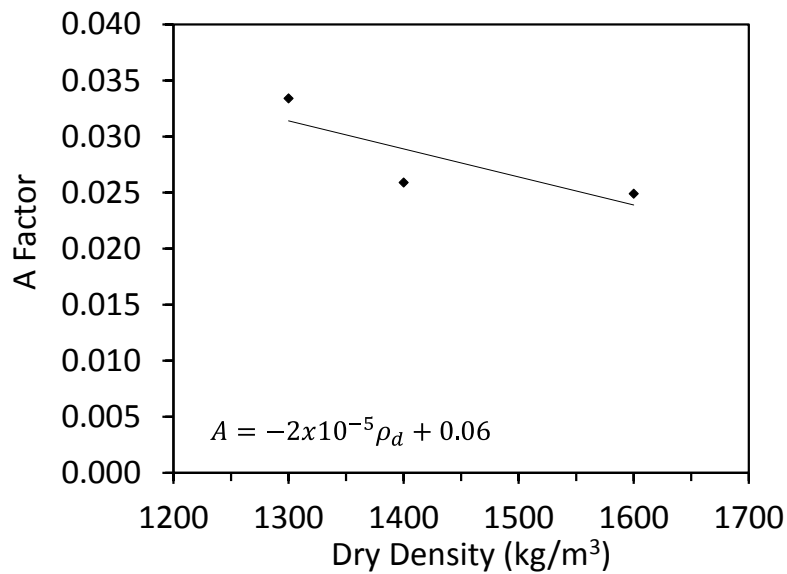


Figure 6.2: The “A” factor (the slope of the linear relationship between dielectric permittivity and volumetric water content) as a function of the initial dry density.

6.3 Impact of the Initial Water Content on the Temperature Effect

The temperature and dielectric permittivity data are plotted against each other in Figure 6.1(a) to evaluate whether the initial water content had an impact on the effect of temperature on the sensor output. Regardless of the initial volumetric water content, a clear linear trend between temperature and permittivity was observed for all of the tests. The increase in volumetric water content is observed to lead to a uniform shift in the temperature effect curves to the right. The change in temperature with the measure change in permittivity is shown in Figure 6.1(b). The slight variations in slope could be due to sensor variability or difference in soil fabric due to compaction at different initial water content values (Mitchell et al. 1965).

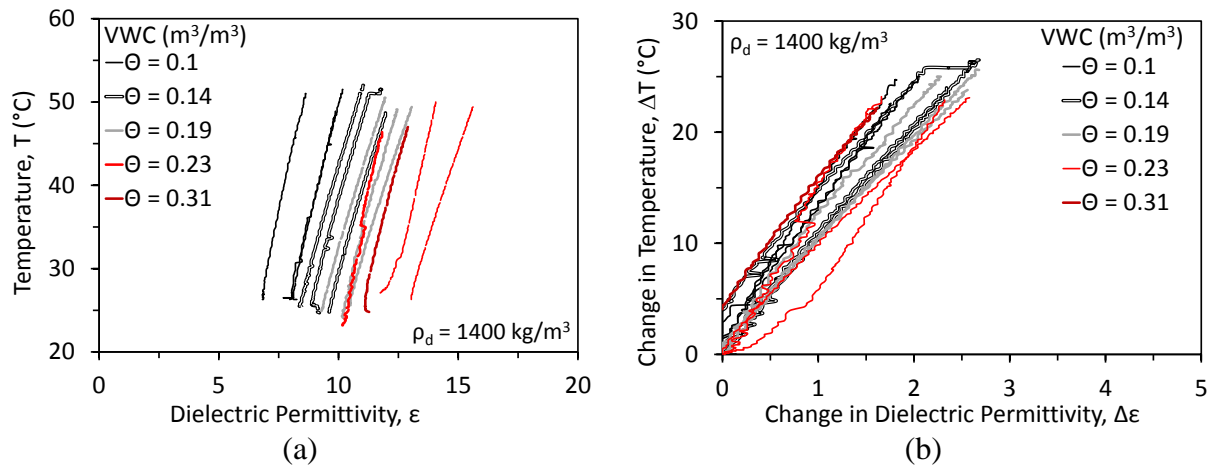


Figure 6.3: Impact of initial water content on the capacitance sensor temperature effects:

(a) Temperature versus apparent dielectric permittivity; (b) Change in temperature versus change in apparent dielectric permittivity.

To better observe any changes in slope between tests of different water contents, the slope of the relationship between dielectric permittivity and the change in temperature for each test was plotted against its initial water content, as shown in Figure 6.4(a). Despite some scatter at a water content of $0.24 \text{ m}^3/\text{m}^3$, there is a slight increasing trend with increasing initial volumetric water content for specimens that all have the same dry density of 1400 kg/m^3 . Although this increase can be expected based on the upper and lower bounds, the magnitude of the increase does not appear to follow the trend expected from the upper and lower bound tests reported in Section 5.2.

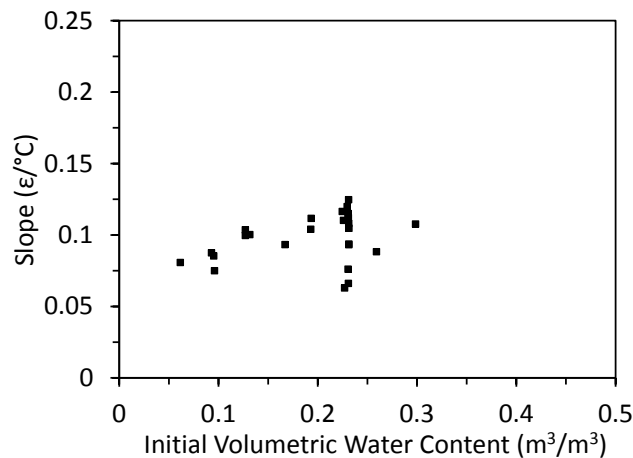


Figure 6.4: Slope of the temperature effect curves for the capacitance sensor for each test plotted against the initial volumetric water content.

6.4 Impact of Initial Dry Density on the Temperature Effect

The temperature and dielectric permittivity data were plotted against each other in Figure 6.5(a) to evaluate whether the initial dry density had an impact on the effect of temperature on the sensor output. A clear linear trend between temperature and permittivity was observed for all of the tests; however the slopes of those lines do appear to vary with dry density. The change in temperature with the measure change in permittivity is shown in Figure 6.5(b). The slopes appear to decrease with increasing dry density. This could be the result of an increased mass of soil and water within the sensor's zone of influence. Overall, it may be concluded that the initial dry density has an impact on the temperature effect on the dielectric sensor output.

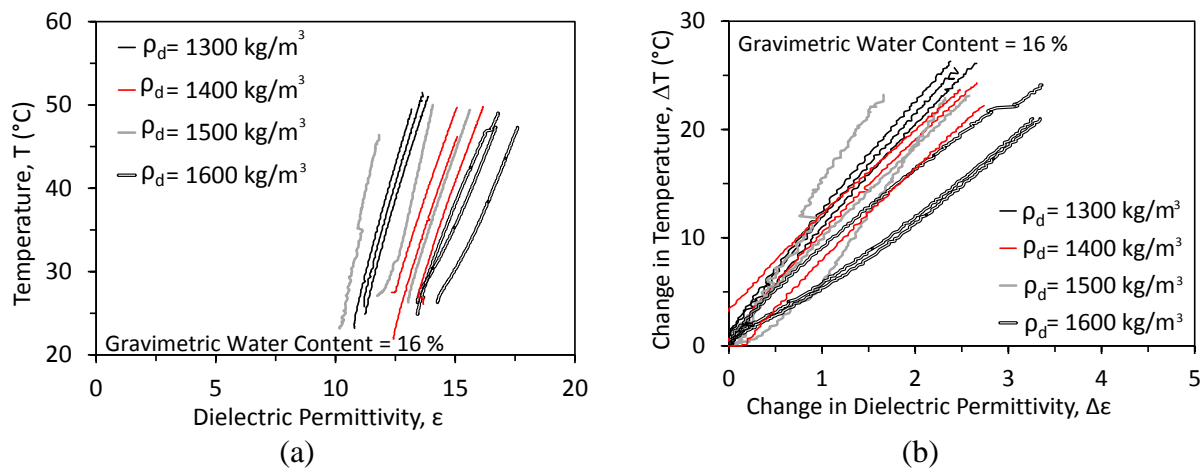


Figure 6.5: Impact of initial dry density on the capacitance sensor temperature effects:

(a) Temperature versus apparent dielectric permittivity; (b) Change in temperature versus change in apparent dielectric permittivity.

To better observe any changes in slope between tests of different dry densities, the rate of change in the dielectric permittivity with change in temperature was again plotted in Figure 6.6. A more significant increase in the rate of change in dielectric permittivity with change in temperature is observed with increasing dry density. The three slopes for the specimens at a dry density of 1500 kg/m^3 do not follow the same trend as the other data, possibly due to the fact

that the sensor response was different than in the other tests (nonlinear trend, shifts in the curves).

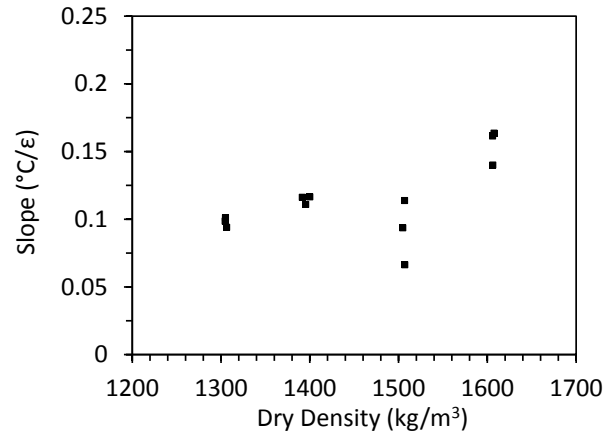


Figure 6.6: The rate of change in dielectric permittivity with change in temperature for each test plotted against the initial dry density.

6.5 Correction Equation for Temperature Effects

As mentioned in Section 6.3, the change in dielectric permittivity as a function of temperature in Figure 6.4 and Figure 6.6 was observed to be relatively linear. Accordingly, a linear calibration equation was developed to remove the effect of temperature on the apparent dielectric permittivity so that the capacitance sensor could be used to evaluate actual changes in volumetric water content during nonisothermal flow processes. The equation has the following form:

$$\varepsilon_{actual} = \varepsilon_{measured} - \Delta T \times m \quad (6.2)$$

where ε_{actual} is the actual dielectric permittivity of the soil without the temperature effect on the sensor, $\varepsilon_{measured}$ is the dielectric permittivity measured using the capacitance sensor, ΔT is the change in temperature, and m is the slope of the temperature effect curve.

The value of m can be defined for a given soil specimen by first accounting for the initial dry density effect, then the initial volumetric water content effect. This approach assumes that the initial volumetric water content effect is the same at the different dry densities, as the effect of

the initial volumetric water content is only available for Bonny silt having a density of 1400 kg/m³. The effects of these two variables on the value of m were determined by applying a linear fit to the data in Figures 6.4 and 6.6, shown as shown in Figures 6.7(a) and 6.7(b), respectively. The data in Figure 6.7(b) includes a best fit line that does not include the data from 1500 kg/m³, which was removed due to issues in how the sensor responded in these tests.

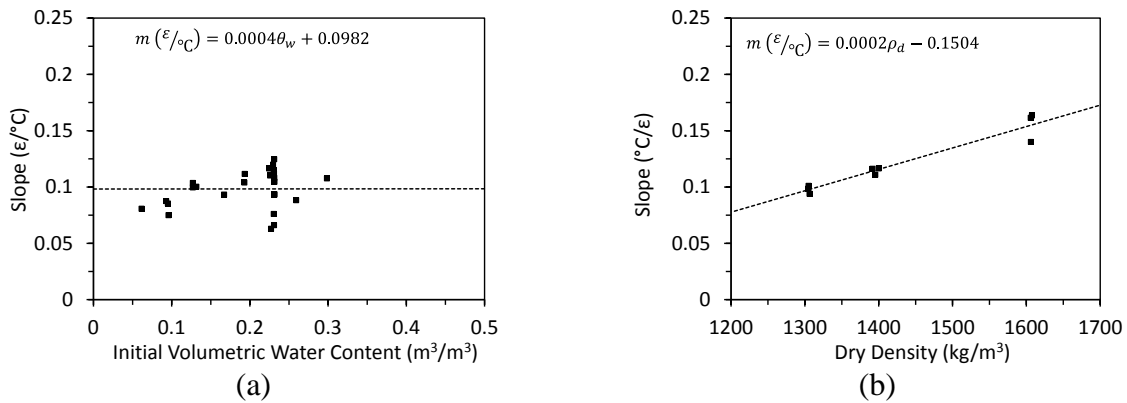


Figure 6.7: The rate of change in dielectric permittivity with change in temperature for each test plotted against the (a) initial volumetric water content and (b) initial dry density.

An example of how the relationships in Figure 6.7 can be used to correct the temperature response of a sensor is shown in Figure 6.8. The three specimens in this test have different initial volumetric water content and dry density values, and the density correction from Figure 6.7(b) was inserted into Equation 6.2. After the correction was applied, the curves show a vertical line, indicating a constant dielectric permittivity with temperature, as expected based on the measured gravimetric water content distributions in these tests.

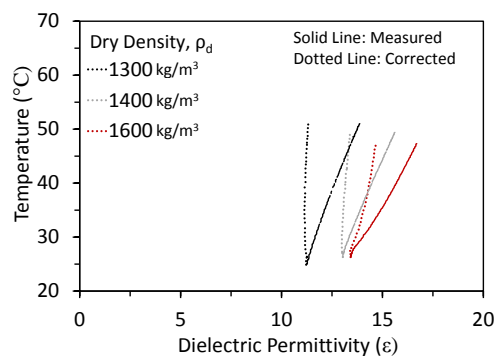


Figure 6.8: Example of the application of the temperature correction equation

CHAPTER 7

CONCLUSION

This study involved an investigation into temperature effects on the response of capacitance sensors used to infer the volumetric water content of unsaturated soils. A compaction mold was modified to characterize the capacitance sensor response during heating, while maintaining a constant water content in the soil. Heating experiments on compacted specimens of Bonny silt with constant water content permitted definition of a calibration equation to consider the soil-specific relationship between volumetric water content and dielectric permittivity. This relationship was defined along with a correction equation to account for temperature effects in unsaturated soils having different dry density values. The following specific conclusions can be drawn from evaluation of the different experiments:

- The temperature effect on the capacitance sensor response was observed to be sensitive to the initial density of the soil and the initial water content of the soil.
- Temperature effects were not noticed on the sensor, heated in dry air, but small changes were noticed in the inferred dielectric measured in oven-dried soil. This suggests that some form of change occurs in the dielectric permittivity of the soil minerals itself, but a much more significant change occurs with the addition of water into the soil matrix. The oven-dried and saturated tests establish boundaries on the temperature effects but the varied initial water content test results suggest there is a constant temperature effect for partially saturated soils that differs from the saturation and oven-dried effects.
- Further experimental research can explore the effect of measurement frequency of the capacitance sensor on the temperature effect in the silt. Further theoretical research can look into the effects of specific surface area and bound water on the temperature effects, which may be encountered in clay soils.

REFERENCES

- Aiban, S.A. and Znidarčić, D. (1989). "Evaluation of the flow pump and constant head techniques for permeability measurements." *Géotechnique* 39, 655-666.
- Assouline, S., Narkis, K., Tyler, S., Lunati, I., Parlange, M., and Selker, J. (2010). "On the diurnal soil water content dynamics during evaporation using dielectric methods." *Vadose Zone Journal*. 9(3), 709-718.
- Bogena, H., Huisman, J., Oberdörster, C., and Vereecken, H. (2007). "Evaluation of a low-cost soil water content sensor for wireless network applications." *Journal of Hydrology*. 344(1-2), 32-42.
- Coccia, C.J.R., Casady, A., and McCartney, J.S. (2013). "Thermo-hydro-mechanical response of unsaturated soils during cyclic heating and cooling." *Proceedings of the 1st Pan-American Conference on Unsaturated Soils*. Feb. 20-22. Cartagena de Indias, Colombia. Taylor and Francis Group, London. 141-146.
- Coccia, C.J.R. and McCartney, J.S. (2013). "Impact of Heat Exchange on the Thermo-Hydro-Mechanical Response of Reinforced Embankments." *Proceedings of GeoCongress 2013*. ASCE. San Diego, CA. Mar. 3-5. pp. 343-352.
- Cobos, D. and Campbell, C. (2013). "Correcting temperature sensitivity of ECH2O soil moisture sensors." *Decagon Devices Application Note*.
- Czarnomski, N., Moore, G., Pypker, T., Licata, J., and Bond, B. (2005). "Precision and accuracy of three alternative instruments for measuring soil water content in two forest soils of the Pacific Northwest." *Canadian Journal of Forest Research*, 35(8), 1867-1876.
- Decagon Devices. (2014). "5TM Water Content and Temperature Sensors." *Operation Manual*. Pullman, WA.

- Evett, S., Tolk, J., and Howell, T. (2006). "Soil profile water content determination." *Vadose Zone Journal*. 5, 894-907.
- Khosravi, A. (2011). *Small Strain Shear Modulus of Unsaturated, Compacted Soils during Hydraulic Hysteresis*. PhD Thesis. University of Colorado Boulder.
- Kizito, F., Campbell, C., Campbell, G., Cobos, D., Teare, B., Carter, B., and Hopmans, J. (2008). "Frequency, electrical conductivity and temperature analysis of a low-cost capacitance soil moisture sensor." *Journal of Hydrology*. 352(2-3), 367-378.
- Liu, Ning. (2007) *Soil and Site Characterization Using Electromagnetic Waves*. PhD. Thesis. Virginia Polytechnic Institute and State University.
- Malmberg and Maryott. (1956.) "Dielectric constant of water from 0°C to 100°C." *Journal of Research of the National Bureau of Standards Research Paper 2641*. 56(1), 1-8.
- Mitchell, J.K., Hooper, D. R., and Campanella, R.G. (1965.) "Permeability of compacted clay." *Journal of the Soil Mechanics and Foundations Division, American Society of Civil Engineers*, Vol. 91, No. SM-4, July. pp. 41-65.
- Murphy, K.D., McCartney, J.S., and Henry, K.H. (2014). "Thermo-mechanical response tests on energy foundations with different heat exchanger configurations." *Acta Geotechnica*. 1-17. DOI: 10.1007/s11440-013-0298-4.
- Nadler, A., Gamliel, A., and Peretz, I. (1999). "Practical Aspects of Salinity Effect on TDR-Measured Water Content." *Soil Science Society of America Journal*, 63(5), 1070-1076.
- Or, D., and Wraith, J. (1999). "Temperature effects on soil bulk dielectric permittivity measured by time domain reflectometry: A physical model." *Water Resources Research*. 35(2), 371-383.
- Pepin, S., and Livingston, N. (1995). "Temperature-dependent measurement errors in time domain reflectometry determinations of soil water." 59(1), 38-43.

- Philip, J., and Vries, D. (1957). "Moisture movement in porous materials under temperature gradients." *Transactions, American Geophysical Union*. 38, 222–232.
- Pozzato, A., Tarantino, A., McCartney, J.S and Zornberg, J.G. (2008). "Effect of dry density on the relationship between water content and TDR-measured apparent dielectric permittivity in compacted clay." *Proceedings of the 1st European Conference on Unsaturated Soils (E UNSAT 2008)*. Durham, UK. Jul. 2-4. Taylor and Francis Group, London. pp. 173-179.
- Roth, K., Schulin, R., Flühler, H., and Attinger, W. (1990). "Calibration of time domain reflectometry for water content measurement using a composite dielectric approach." *Water Resources Research*. 26(10), 2267-2273.
- Rothe, A., Weis, W., Kreutzer, K., and Matthies, D. (1997). "Changes in soil structure caused by the installation of time domain reflectometry probes and their influence on the measurement of soil moisture." 33(7), 1585-1593.
- Seyfried, M., and Grant, L. (2007). "Temperature effects on soil dielectric properties measured at 50 MHz." *Vadose Zone Journal*, 6(4), 759–765.
- Smits, K.M., Sakaki, T., Howington, S.E., Peters, J.F. & Illangasekare, T.H. (2013). "Temperature dependence of thermal properties of sands over a wide range of temperatures [30-70°C]." *Vadose Zone Journal*. 12(1), 1-8. doi:10.2136/vzj2012.0033.
- Stewart, M.A., Coccia, C.J.R., and McCartney, J.S. (2014). "Issues in the implementation of sustainable heat exchange technologies in reinforced, unsaturated soil structures." *Proceedings of GeoCongress 2014 (GSP 234)*, M. Abu-Farsakh and L. Hoyos, eds. ASCE. 4066-4075.
- Topp, G., Davis, J., and Annan, A. (1980). "Electromagnetic determination of soil water content: Measurements in coaxial transmission lines." *Water Resources Research*. 16(3), 574–582.

- van Genuchten, M.T. (1980). "A closed-form equation for predicting the hydraulic conductivity of unsaturated soils." *Soil Science Society of America Journal*. 44(5), 892–898.
- Wraith, J., and Or, D. (1999). "Temperature effects on soil bulk dielectric permittivity measured by time domain reflectometry: Experimental evidence and hypothesis development." *Water Resources Research*, 35(2), 361–369.
- Wraith, J., Or, D., and Jones, S. (2001). "Dielectric properties of bound water: Application to porous media surface area and grain moisture determination." *TDR 2001: Proceedings of the Second International Symposium and Workshop on Time Domain Reflectometry for Innovative Geotechnical Applications*. Northwestern University, September 5-7, 2001, Evanston, Illinois.